Made available by Hasselt University Library in https://documentserver.uhasselt.be

Spatial analysis of the rice leaf growth zone under controlled and cadmium-exposed conditions

Peer-reviewed author version

HUYBRECHTS, Michiel; HENDRIX, Sophie; Bertels, J; Beemster, GTS; VANDAMME, Dries & CUYPERS, Ann (2020) Spatial analysis of the rice leaf growth zone under controlled and cadmium-exposed conditions. In: Environmental and Experimental Botany, 177 (Art N° 104120).

DOI: 10.1016/j.envexpbot.2020.104120
Handle: http://hdl.handle.net/1942/31916

Spatial analysis of the rice leaf growth zone under controlled and cadmium-exposed conditions

Michiel Huybrechts[1], Sophie Hendrix[1], Jonas Bertels[2], Gerrit T.S. Beemster[2], Dries Vandamme[3], Ann Cuypers[1]*

[1] Environmental Biology, Centre for Environmental Sciences, Hasselt University, B-3590 Diepenbeek, Belgium

[2] Laboratory for Integrated Molecular Plant Physiology Research (IMPRES), Department of Biology, University of Antwerp, 2020 Antwerp, Belgium

[3]Applied and Analytical Chemistry, Centre for Environmental Sciences, Hasselt University, B-3590 Diepenbeek, Belgium

*Correspondence: ann.cuypers@uhasselt.be

Abstract

Worldwide contamination of agricultural soils with cadmium (Cd) not only leads to reduced plant yield, but accumulation within the edible plant parts also poses a serious threat to human health. In this study, the rice leaf growth zone was used to examine how the effects of Cd on leaf growth are mediated by its effect on cell division and expansion. Based on a kinematic analysis and flow cytometry, we show that both processes are inhibited upon root Cd exposure. The Cd-inhibited leaf growth was confirmed by the overall downregulation of cell cycle genes upon Cd exposure. In addition, Cd preferentially accumulates within the leaf meristem and the transition zone, whereas the concentration steeply drops in the elongation zone. As Cd induces an oxidative challenge, which is also related to plant growth, it was

further investigated whether this could be involved in the mode of action of the Cd-inhibited leaf growth. Therefore, gene expression patterns of antioxidative enzymes such as superoxide dismutases (SOD), catalases (CAT) and ascorbate peroxidases (APX) were investigated in different leaf growth zones. Whereas no significant differences were seen for *SOD* expression across the different leaf zones under control conditions, large differences in abundance were visible for *APX* and *CAT* expression. Moreover, Cd stress significantly upregulated genes in these families in an isoform- and location-dependent fashion, indicating the possible involvement of the Cd-induced oxidative challenge in regulating leaf growth processes and highlighting the importance of specific leaf sampling for further investigations.

Keywords

Antioxidative defense, Cadmium, Cell cycle, Leaf growth, Oxidative stress, Rice

Abbreviations

APX	Ascorbate peroxidase
Ca	Calcium
CAT	Catalase
Cd	Cadmium
CDKB1;1	Cyclin-dependent kinase B1-1
CDKB2;1	Cyclin-dependent kinase B2-1
CYCA3;2	Cyclin-A3-2
D	Division zone
DAPI	4′-6-diamino-phenolindole
DW	Dry weight
E	Elongation zone
FLL	Final leaf length

Fe	Iron
H_2O_2	Hydrogen peroxide
LER	Leaf elongation rate
l_{mat}	Mature cell length
M	Maturation zone
MIQE	Minimum Information for publication of qPCR Experiments
mRNA	Messenger-RNA
$O_2^{\bullet-}$	Superoxide
$^{\bullet}OH$	Hydroxyl radical
PAR	Photosynthetic active radiation
PI	Propidium iodide
PSB	Pellet Solubilization Buffer
RBR2	Retinoblastoma-related protein 2
ROS	Reactive oxygen species
T_1	Transition zone 1
T_2	Transition zone 2
SOD	Superoxide dismutase
UPB1	UPBEAT1
Zn	Zinc

1. Introduction

Worldwide contamination of agricultural soils with metals may cause severe health threats due to metal accumulation in the food chain. In China, 16.1% of arable land is polluted with inorganic pollutants, cadmium (Cd) being the most prominent (Duan *et al.*, 2016). Rice, which is a stable food source for over half the world's population, tends to accumulate more Cd than other cereals (Hu *et al.*, 2016a). As a non-essential plant element, Cd enters via

transporters intended for essential nutrients such as iron (Fe), zinc (Zn) and calcium (Ca) (Clemens and Ma, 2016; Kabata-Pendias and Pendias, 2001; Loix *et al.*, 2017). After absorption in the roots, the Cd ions are translocated to the rice shoot and eventually remobilized to the grains (Rizwan *et al.*, 2016). Plants exposed to Cd show symptoms of growth retardation, reduced photosynthetic activity and impaired nutrient homeostasis (Cuypers *et al.*, 2009; Sandalio *et al.*, 2001). At the physiological level, Cd is known to induce oxidative stress in an indirect manner by elevating the production of reactive oxygen species (ROS) and/or reducing the antioxidant defense, thereby possibly damaging macromolecules such as lipids, DNA and proteins (Cuypers *et al.*, 2010). Under non-stressful conditions, ROS are produced in chloroplasts during photosynthesis, during mitochondrial respiration, in photorespiratory reactions in the peroxisomes and by apoplastic NADPH oxidases (Mhamdi and Van Breusegem, 2018). A plethora of antioxidative mechanisms have evolved in plants to ensure that ROS levels are kept at a basal level (Cuypers *et al.*, 2016; Mittler, 2017). Recent reviews have highlighted the important role of ROS in normal plant growth and development (Huybrechts *et al.*, 2019; Mhamdi and Van Breusegem, 2018). In a recent study using 13 maize varieties with different drought sensitivity, it was shown that the leaf elongation rate (LER) was less affected under drought stress in the tolerant lines (Avramova *et al.*, 2017). Furthermore, these tolerant maize lines had higher antioxidant levels and higher activities of redox-regulating enzymes such as catalase (CAT) and ascorbate peroxidase (APX) suggesting a link between antioxidant regulation and leaf growth. Moreover, overexpression of the *Arabidopsis thaliana* iron-superoxide dismutase (SOD) in maize leads to a higher extent of cell division in the leaf growth zone and results in increased leaf growth (Avramova *et al.*, 2015a). In *A. thaliana* root tips, exogenous application of hydrogen peroxide (H_2O_2) affected the expression of cell cycle-related genes (Tsukagoshi, 2012). Moreover, the transition between cell proliferation and elongation in the root tips was

accompanied by a shift from superoxide ($O_2^{\bullet-}$) accumulation in the meristem to elevated levels of H_2O_2 in the elongation zone (Tsukagoshi *et al.*, 2010). This ROS separation was achieved by the transcription factor UPBEAT1 (UPB1) through regulating the expression of peroxidases. UPB1 was also suggested to be involved in cell wall remodeling through ROS activity as indicated by a genome-wide profiling study. As a major determinant of leaf growth, cell wall expansion can also in part be regulated by ROS homeostasis (Schmidt *et al.*, 2016). Hydroxyl radicals ($^{\bullet}OH$) were found to stimulate cell wall loosening through the cleavage of the hemicellulose xyloglucan or pectin (Müller *et al.*, 2009). In contrast, H_2O_2 induces crosslinking of phenolic side chains of the cell wall, leading to a reduced cell wall extensibility (Schopfer, 1996). Another transcription factor, KUODA1, was shown to inhibit the expression of cell wall-located peroxidases in the leaves of *A. thaliana*, thus keeping H_2O_2 levels in the apoplast low and promoting cell expansion (Lu *et al.*, 2014). Finally, early chloroplast differentiation and the start of photosynthetic ROS production along the leaf axis might also serve as a signal for cells to arrest cell proliferation (Andriankaja *et al.*, 2012; Schippers *et al.*, 2016).

Still very little research is done on how ROS and plant growth regulation are interconnected and even much less on how Cd-induced oxidative stress can perturb the processes of cell proliferation and expansion. Cell suspension cultures of soybean exposed to a Cd range from 1 to 10 µM, showed a downregulation of the mRNA levels of cyclin B1 after exposure to more than 6 µM Cd (Sobkowiak and Deckert, 2003). Cell cycle progression was also retarded after exposure for 7 and 11 days to 0.2 mM $Cd(NO_3)_2$ in roots of rice seedlings and abscisic acid was shown to regulate the expression of several cell cycle genes (Zhao *et al.*, 2014). Recently, in leaves of *A. thaliana*, cell cycle progression and endoreplication were inhibited upon short-term exposure to 5 µM Cd during 72 h. This response was hypothesized to be due

to oxidative stress and subsequent induction of the DNA damage response that is associated with cell cycle regulation (Hendrix *et al.*, 2018).

Besides being a major food source for half of the world's population, rice is an important model organism for monocots. As a grass, the leaves grow in a characteristic linear manner, which results in cells dividing at the leaf base, expanding in the elongation zone and finally reaching their final size in the maturation zone (Sprangers *et al.*, 2016). The spatial patterning of these leaf zones remains constant during a short period of steady-state growth that occurs around leaf appearance in case of rice (Parent *et al.*, 2009). In this steady-state phase of leaf growth, processes of cell division and expansion are separated along the leaf axis. By mapping these leaf zones, high resolution sampling can support the research to unravel the Cd-induced processes that interfere with plant growth (Avramova *et al.*, 2015b).

In this study, we combined kinematic analysis of the leaf growth zone with flow cytometry and gene expression analysis on different locations of the leaf growth zone in control and Cd-exposed plants. The focus was on (1) the Cd-inhibited leaf growth and its relation to the expression of cell cycle genes within the different leaf growth zones and (2) the possible involvement of antioxidative genes in controlling leaf growth and development.

2. Materials and methods

2.1. Plant material, growth conditions and Cd exposure

Oryza sativa L. cv. Nipponbare seeds (GSOR-100, United States Department of Agriculture) were surface-sterilized with a 0.1% bleach solution and placed in water for imbibition for 24 h. After this period, the seeds were placed on filter paper in petri dishes for 3 days to stimulate germination. Germinated seeds were transferred to a hydroponic culture adapted from the one described for *A. thaliana* by Smeets *et al.* (2008). The rice plants received a full-strength Kimura B nutrient solution (pH 5.5-5.6) that was renewed twice a week (Yoshida *et al.*,

1971). The climate chamber was set at 65% relative humidity, 16 h/8 h photoperiod and 28/23 °C day/night temperatures. Light was generated by Philips Green-Power LED-modules consisting of red, far red and blue units providing photosynthetic active radiation (PAR). The PAR at plant level was set at 170 µmol m^{-2} s^{-1}. At the time of appearance of the fourth leaf, the plants were exposed to 10 or 50 µM Cd by adding $CdSO_4$ to the nutrient solution or continued to grow under controlled conditions. The concentrations used in this study were 10 µM Cd, which led to growth reduction and, 50 µM Cd, which caused a nearly complete growth arrest. Because Cd delayed the appearance of the sixth leaf, it was opted to harvest the plants at the same developmental stage. Therefore Cd-exposed plants were harvested respectively one and four days later for the 10 and 50 µM Cd condition than the control condition.

2.2. Leaf length measurements

After the fourth leaf emerged from the whorl of older leaves, leaf length was followed up for 10 plants of each condition until the sixth leaf reached its final leaf length (FLL). The lengths of the fourth, fifth and sixth leaf were daily measured at the same time in the morning with a ruler. Since leaf six developed completely under Cd exposure, all other measurements were performed on this leaf.

2.3. Kinematic analysis

In order to obtain a detailed view of the leaf growth zone, a full kinematic analysis based on microscopy was performed according to Fiorani and Beemster (2006), with minor modifications for rice leaves. One day after appearance of the sixth leaf, the leaves of five plants were separated and the first five centimeters of the sixth leaf base were covered with transparent nail polish. After five minutes, the nail polish was removed using cellophane tape and placed on a microscope slide. The imprint was further analyzed with a Leica DM 2500

light microscope. A picture of every millimeter of the imprint was taken with a Leica DFC450 C camera connected to the microscope. These pictures were later analyzed with ImageJ software (Schneider *et al.*,2012), which allowed cell length measurements. The cells flanking the stomatal cell files were used to perform these measurements to track the same cell type throughout the growth zone. The raw data of individual leaves were smoothed using the kernel smoothing function locpoly of the Kern Smooth package (Wand and Jones, 1995) created for R statistical software (R Core Team, 2014).

2.4. DAPI staining of the meristem

After an imprint of the leaf base was made for microscopic analysis, the lower two centimeters were cut off and placed in a 3:1 (v:v) absolute ethanol:acetic acid solution. These samples were placed at 4 °C and kept in the dark for a minimum of 24 h before analysis. The samples were soaked in a buffer (50 nM NaCl, 5 mM EDTA and 10 mM TRIS pH 7) for 20 minutes. Next, they were stained for 5 minutes with a 4',6-diamidino-2-phenylindole (DAPI) staining solution (same buffer as above supplemented with 1 µg ml^{-1} DAPI) and mounted on a microscope slide. The fluorescent signals coming from epidermal cells were observed in the dark with a fluorescent microscope using UV-excitation (Leica DM 2500 LED). Based on the observation of the most distal dividing nuclei, an estimation of the length of the leaf meristem was made.

2.5. Flow cytometric analysis

To further investigate the effect of Cd on the leaf growth zones of rice plants, flow cytometry was performed on the sixth leaf. The growth zone of individual plants was cut evenly in 10 segments of 5 mm size and snap frozen in liquid nitrogen. The leaf samples were chopped with a sharp razor blade in 500 µL nuclei extraction buffer and subsequently filtered through a 50 µm nylon filter (CellTrics®, Sysmex Partec). The DNA was stained using 2 mL staining

194 solution containing staining buffer, propidium iodide (PI) and RNase. The products were
195 included in the CyStain® PI Absolute P kit (Sysmex Partec). After 1 h of incubation on ice
196 and in the dark, the samples were analyzed with a CyFlow Cube 8 (Sysmex Partec). Samples
197 were run until a threshold of 10.000 nuclei was reached. Nuclei were excited using a 488 nm
198 laser and the forward scatter and PI fluorescence intensity (FL-2 channel; 580/30 nm) were
199 measured. Flow cytometry plots were analyzed using FCS Express 6 software (De Novo
200 Software). At least five plots from individual plants were merged per location to get a detailed
201 view of the cell cycle responses.

202 **2.6. Determination of Cd accumulation**

203 According to the data obtained from the kinematic analysis, the leaf growth zone of the sixth
204 leaf was divided into five different zones; the division zone (D), transition zone 1 (T_1),
205 elongation zone (E), transition zone 2 (T_2) and maturation zone (M). To determine the Cd
206 concentration, these five zones were harvested, and in addition a 1 cm part of the leaf blade
207 was taken at 1 cm from the top. The leaf segments were placed in a -20 °C freezer for 1 h and
208 immediately afterwards vacuum dried in a lyophilizer. Next, the samples were fully digested
209 at 110 °C using 69% HNO_3 (ARISTAR® for trace analysis) for three times and the fourth time
210 using 37% HCl (ARISTAR® for trace analysis) in a heat block until the samples were
211 completely dry. Finally, the samples were dissolved in 2% HCl (diluted with milliQ H_2O).
212 The Cd concentration was quantified using inductively coupled plasma mass spectrometry
213 (ICP-MS) using a NexION 350S (Perkin Elmer) based on an 11-points calibration curve (R^2 =
214 0.999994 for Cd114) and using indium as internal standard.

215 **2.7. Gene expression analysis**

216 Five segments from the sixth leaf growth zone of both control and 10 µM Cd-exposed plants
217 were snap frozen in liquid nitrogen and stored in a -80 °C freezer till further analysis. For

RNA extraction, samples were pulverized with stainless steel beads in a Retsch Mixer Mill MM 400. To the pulverized sample, 400 µL Pellet Solubilization Buffer (PSB) consisting of 7M Guanidine HCl, 2% (v/v) TWEEN 20, 4% (v/v) NP-40, 50 mM Tris, pH 7.5 and 1% (v/v) ß-mercaptoethanol were added (Valledor *et al.*, 2014). Next, the samples were incubated for 15 min at 28 °C and centrifuged at 14000 g for 3 min. The supernatant was transferred to a new silica column and centrifuged at 10000 g for 1 min. Afterwards, 200 µL PSB buffer was added to the column and again centrifuged at 12000 g for 2 min. The silica column was discarded and 300 µL acetonitrile was added to the Eppendorf. This solution was transferred onto a new silica column and centrifuged at 12000 g for 2 min. The column was subsequently washed with 600 µL of buffer 1 (2 mM Tris pH 7.5, 20 mM NaCl, 0.1 mM EDTA, 90% ethanol) and 600 µL of buffer 2 (2 mM Tris pH 7.5, 20 mM NaCl, 0.1 mM EDTA, 70% ethanol) alternate with centrifugation at 12000 g for 2 min. To elute the RNA from the column, 50 µL RNA free H_2O was added to the filter. The concentration and purity of the extracted RNA were determined using a NanoDrop® ND-1000 spectrophotometer (Thermo Fisher Scientific). Afterwards, possible remaining DNA was removed with the TURBO DNA-free™ Kit (Ambion, Thermo Fisher Scientific). For each sample, a standardized 1 µg RNA input was used for reverse transcription by the PrimeScript™ RT Reagent Kit, according to the manufacturer's instructions (Perfect Real Time, Takara Bio Inc., Kusatsu, Japan). The final cDNA product was 1/10 diluted in TE buffer (1 mM Tris-HCl, 0.1 mM EDTA, pH 8.0) and stored at −20 °C before further analysis. Quantitative Real-time PCR was performed with a 7500 Fast Real-Time PCR System (Applied Biosystems, Thermo Fisher Scientific). From the diluted cDNA samples, 2 µL was added to 5 µL QuantiNova SYBR® Green (Qiagen), 0.05 µL QN ROX Reference Dye, 2.35 µL RNase-free H_2O and 0.3 µL of both forward and reverse primer (sequences available in Supplemental Table A1). Amplification occurred using standard cycling conditions (2 min at 95 °C, 40 cycles of 5 s at

95 °C and 10 s at 60 °C). A dissociation curve was generated to validate product specificity. Relative gene expression levels were determined using the $2^{-\Delta Cq}$ method, relative to the sample with the highest expression (smallest Cq value). Based on the GrayNorm algorithm developed by Remans *et al.* (2014), the data were normalized using the expression levels of the following reference genes: *EUKARYOTIC INITIATION FACTOR 4A-3* (*eIF4A-3*), *NONSENSE-MEDIATED DECAY UPF3* (*UPF3*), *EUKARYOTIC ELONGATION FACTOR 1A* (*eEF-1α*) and *EXPRESSED PROTEIN (EXPnarsai).* Forward and reverse primers were designed in Primer3 or adapted from another study as shown in Supplemental Table A1. Primer specificity was validated for the rice genome using the NCBI BLAST tool (https://blast.ncbi.nlm.nih.gov/Blast.cgi). Primer efficiencies were calculated based on a two-fold dilution series standard curve of two pooled samples from control and Cd-exposed plants. Only primers with an efficiency between 80 and 120% were used for qPCR analysis. Supplemental Table A2 shows qPCR parameters as defined by the Minimum Information for publication of qPCR Experiments (MIQE) guidelines (Bustin *et al.*, 2009).

2.8. Statistical analysis

All statistical tests were performed using the R software version 3.4.2 (R Core Team, 2014). Datasets were tested for normality and homoscedasticity using the Shapiro-Wilk and the Bartlett's test, respectively. When one or both assumptions were violated, the dataset was transformed (inverse, square root, exponent or logarithm). The gene expression data were always log-transformed. Depending on the number of variables, a one-way or two-way ANOVA was performed, followed by a post-hoc Tukey's HSD test. If the transformed data also did not meet the assumption of normality, the non-parametric Kruskal-Wallis test was performed, followed by the Wilcoxon rank sum test. Gene expression data outliers were detected using the Extreme Studentized Deviate method (GraphPad software) at significance level 0.05 and removed from the dataset.

3. Results and discussion

3.1. Cadmium-exposed rice plants show biomass reduction and shorter leaf lengths

In order to study the effect of Cd on leaf growth, we exposed rice seedlings grown in a hydroponic culture system to 10 and 50 µM $CdSO_4$ when the fourth leaf appeared out of the whorl of older leaves. When the sixth leaf appeared, both the stem and roots were weighed. The biomass of Cd-exposed plants was affected in a concentration-dependent manner (Fig. 1A). The weight of the stem showed a 24% and 39% reduction for the exposure to 10 and 50 µM Cd respectively when compared to the control plants (Fig. 1B). The roots were more strongly affected, with a 30% and 49% weight reduction under similar conditions (Fig. 1C). Dose-dependent effects of Cd on plant biomass were also observed in other plant species such as *Brassica juncea* and *A. thaliana* (Ahmad *et al.*, 2011; Keunen *et al.*, 2011). Adverse effects on plant growth and biomass production can however be highly variable between different species and are dependent on Cd concentration and exposure duration (Rizwan *et al.*, 2017). In a study with *Helianthus annuus*, the root biomass was more strongly reduced than the leaf biomass after 4 days of 20 µM $CdCl_2$ exposure (Saidi *et al.*, 2014). On the contrary, in pea plants, the leaves showed the strongest dry weight reduction, with a significant drop already at 20 µM $CdCl_2$, while a significant decrease for the roots was only found at 50 µM $CdCl_2$ and not at lower Cd concentrations (Sandalio *et al.*, 2001). To conclude, our results indicate that the root biomass is more reduced by Cd exposure than the leaf biomass for rice plants grown in our experimental setup.

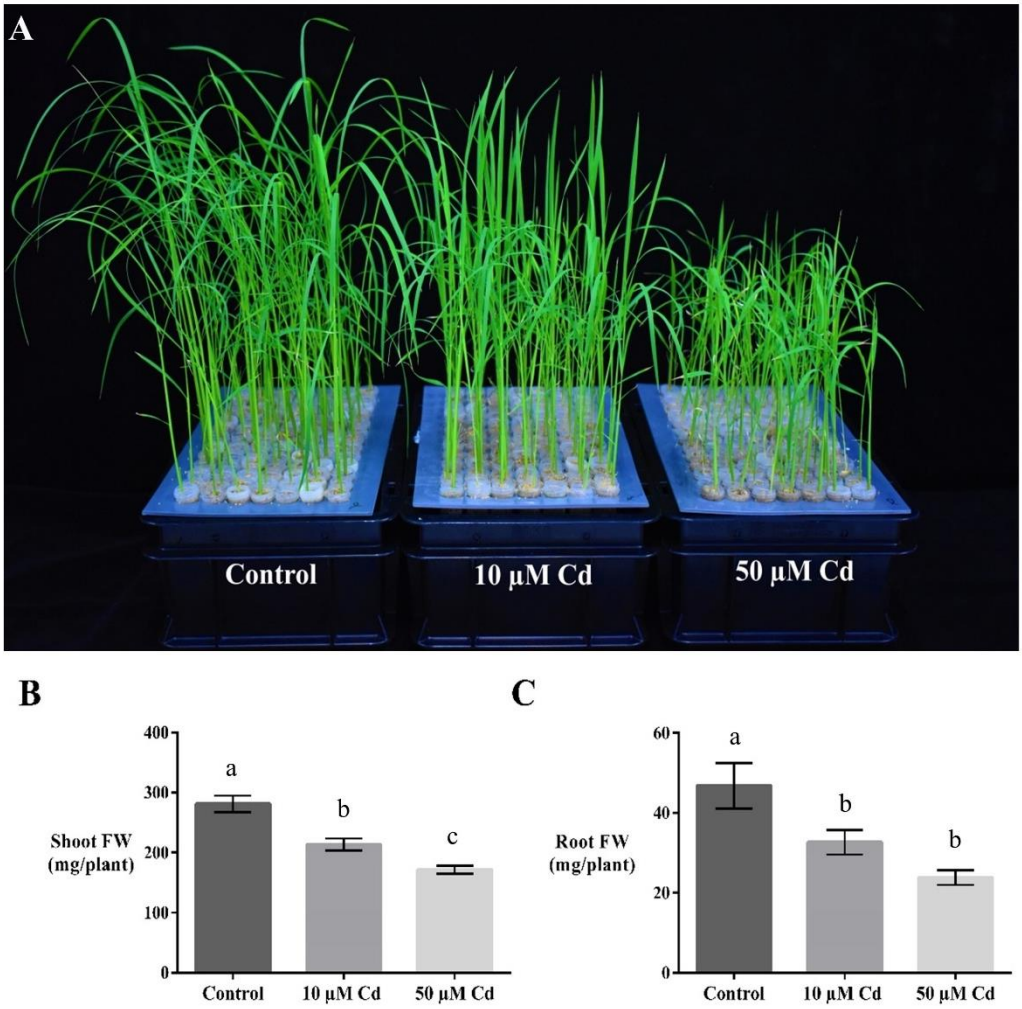

289

290 **Fig 1. A.** *Oryza sativa* L. cv. Nipponbare control and Cd-exposed plants at appearance of the sixth
291 leaf. **B-C.** Shoot fresh weight (**B**) and root fresh weight (**C**). Data given represents the mean ± S.E. of
292 at least 14 plants. Different letters indicate significant differences between groups (One-way ANOVA,
293 p-value < 0.05).

294 In addition, the leaf lengths were daily measured for three successive leaves until the sixth
295 leaf had reached its final leaf length (FLL) (Fig. 2). For control plants, the length of younger
296 leaves surpassed the length of older leaves. Typically, LER of already present leaves drops
297 very quickly, when a younger leaf emerges. This is in accordance with findings from Parent
298 and colleagues (2009) and a demonstration of the self-regulating dynamic system by which
299 emerging leaves of grasses control the leaf elongation of the older one (Fournier *et al.*, 2005;
300 Parent *et al.*, 2009). For plants exposed to 10 µM Cd, the fifth leaf had almost the same length

301 as the fourth leaf, respectively 25.9 and 26.3 cm, yet the sixth leaf was again significantly
302 longer with a length of 29.2 cm. Leaves from plants exposed to 50 µM Cd were most strongly
303 affected in terms of FLL ranging from 21.2 cm for the fourth leaf, 15.4 cm for the fifth leaf to
304 12.9 cm for the sixth leaf. These data suggest that plants were able to adapt to the lowest Cd
305 concentration, but not to the 50 µM Cd concentration. Studies concerning the effect of abiotic
306 stress on successive leaves are scarce. In rice plants exposed to 50 mM NaCl, leaves
307 developing just after exposure showed little effect but a decrease in leaf length became more
308 pronounced for later emerging leaves after prolonged exposure (Yeo *et al.*, 1991). In addition,
309 wheat plants grown in soil with high mechanical resistance for the roots, showed a reduction
310 of leaf elongation and FLL, especially in the youngest leaf (Beemster and Masle, 1996).

311 Besides a reduction in leaf size, also the time of leaf appearance was affected in the most
312 severe Cd exposure condition. The fifth leaf had a delayed appearance of one day and the
313 sixth leaf appeared even four days later compared to the control plants (Fig. 2). This
314 observation was taken into account in sampling for further detailed growth and molecular
315 analysis and therefore, samples were harvested on different days according to the Cd
316 concentration to which the plants were exposed so that they were in the same developmental
317 stage.

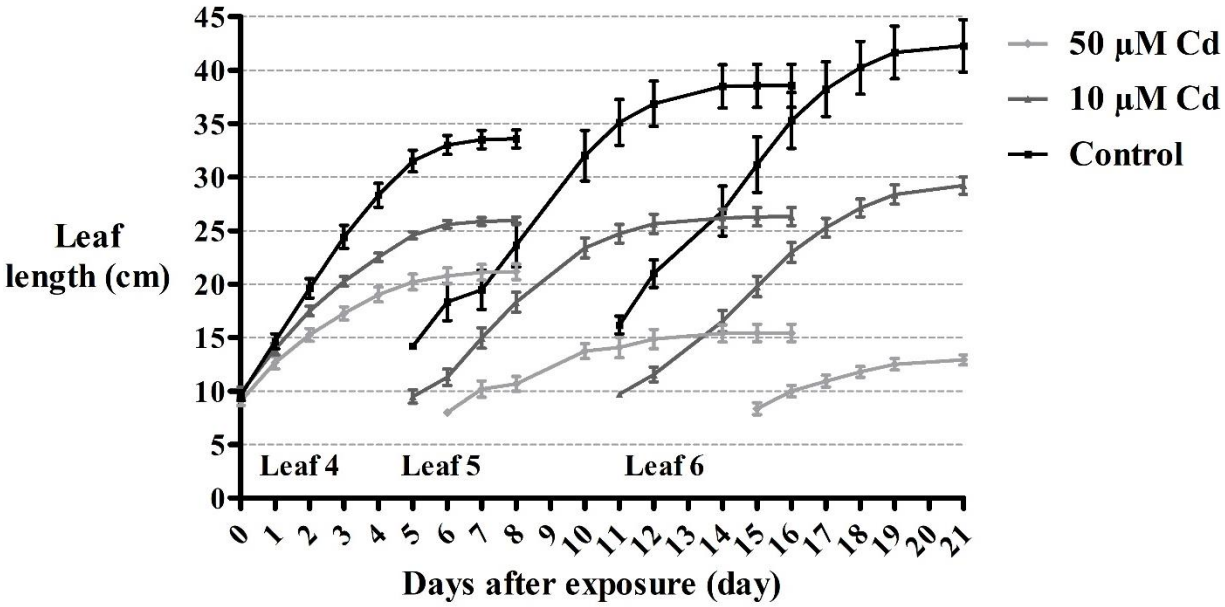

Fig 2. Leaf length progression of leaves 4 to 6 after Cd exposure at leaf 4 appearance. Leaf length was monitored from the moment of appearance out of the whorl of older leaves until the FLL was reached. Data represent the mean ± S.E. of at least 8 plants.

3.2. Kinematic analysis of the leaf growth zone reveals that Cd reduces the meristem size and mature cell length

In order to determine the cellular basis of leaf growth reduction, a kinematic analysis was performed on the sixth leaf. In a meta-analysis across species, the FLL was shown to be mostly dependent on the LER which accounted for 94% of the variation in FLL, while duration of the growth process was of less significance (Gazquez and Beemster, 2017). In this study, the LER was calculated by taking the change between the leaf length at appearance and the leaf length one day later. The leaf growth rate of plants exposed to 50 µM Cd was reduced by 42% compared to the control plants ($P < 0.01$), whereas plants exposed to 10 µM Cd also showed a decreasing trend (18%), although not significant (Table 1).

Table 1. Comparison between kinematic parameters of the sixth leaf between control and Cd-exposed plants. The percentage reduction compared to the control is given in a separate column next to each

condition. Different letters indicate significant differences (One-way ANOVA or Kruskal-Wallis test, p-value < 0.05). Values represent the mean ± S.E. of 5 plants.

Parameters	Control	10 µM Cd	%	50 µM Cd	%
Leaf elongation rate (mm.h^{-1})	2.34 ± 0.26 **a**	1.92 ± 0.11 **a**	**-18**	1.36 ± 0.11 **b**	**-42**
Mature cell length (µm)	66.14 ± 3.16 **a**	55.59 ± 1.27 **b**	**-16**	52.35 ± 1.78 **b**	**-21**
Cell production (cells.h^{-1})	36 ± 4 **a**	34 ± 2 **a**	**-6**	26 ± 2 **a**	**-28**
Cell division rate (cells.cells^{-1}.h^{-1})	0.08 ± 0.01 **a**	0.10 ± 0.01 **a**	**+25**	0.11 ± 0.02 **a**	**+38**
Cell cycle duration (h)	8.89 ± 0.81 **a**	7.21 ± 0.63 **a**	**-19**	7.28 ± 0.98 **a**	**-18**
Residence time in the meristem (h)	77.72 ± 6.66 **a**	61.21 ± 5.88 **a**	**-21**	58.74 ± 8.34 **a**	**-24**
Meristem size (mm)	4.81 ± 0.19 **a**	3.84 ± 0.13 **b**	**-20**	2.82 ± 0.17 **c**	**-41**
Number of cells in the meristem (cells)	437 ± 24 **a**	354 ± 28 **ab**	**-19**	264 ± 26 **b**	**-40**
Size of cells leaving the meristem (µm)	13.65 ± 1.13 **a**	12.61 ± 1.12 **a**	**-8**	13.10 ± 0.73 **a**	**-4**
Average expansion rate (µm.µm^{-1}.h^{-1})	0.06 ± 0.01 **a**	0.07 ± 0.01 **a**	**+17**	0.07 ± 0.01 **a**	**+17**
Residence time in the elongation zone (h)	29.33 ± 5.82 **a**	22.70 ± 3.11 **a**	**-23**	22.33 ± 3.25 **a**	**-24**
Number of cells in the elongation zone (cells)	950 ± 100 **a**	759 ± 71 **ab**	**-20**	561 ± 69 **b**	**-40**
Size of the growth zone (mm)	31 ± 2.32 **a**	23.6 ± 0.46 **ab**	**-24**	18.2 ± 1.97 **b**	**-41**
Number of cells in the growth zone (cells)	1387 ± 98 **a**	1113 ± 77 **a**	**-20**	825 ± 83 **a**	**-41**

At the cellular level, leaf growth is in essence the result of two processes namely cell division determining the number of cells produced in the meristem per unit of time and cell expansion determining the mature cell length (l_{mat}) reached at the end of the elongation zone (Avramova *et al.*, 2017). Since Cd induces a decrease in LER in a dose-dependent manner, at least one of these two parameters must be affected. Therefore, we determined cell length distribution along the leaf axis of Cd-exposed plants, which showed a distinct pattern when compared to control plants (Fig. 3A). Firstly, l_{mat} was reduced by 16 and 21% for 10 and 50 µM Cd, respectively ($P < 0.05$). Mature cell length is determined by the size of the cells leaving the meristem, the time they spend in the elongation zone and the average cell expansion rate

(Sprangers *et al.*, 2016). None of these parameters was significantly affected by Cd separately, but a clear decreasing trend in the duration cells spend in the elongation zone is the most likely explanation for the reduced mature cell size. In maize plants, l_{mat} is often unaffected under different abiotic stresses as a lowered cell expansion rate is compensated for by a longer residence time in the elongation zone, resulting in similar sized cells at the end of the growth zone (Avramova *et al.*, 2015a; Fina *et al.*, 2017; Rymen *et al.*, 2007). In rice, a similar compensation mechanism might be present, since in rice plants overexpressing the *KRP1* cell cycle inhibitor, a reduced cell production was offset by larger mature epidermal cells (Barroco *et al.*, 2006). However, several other studies found similarly affected mature cell sizes (15-25%), suggesting that the effect of abiotic stress may depend on experimental conditions including species, stress treatment and duration (Beemster *et al.*, 1996; Nelissen *et al.*, 2018; Tardieu *et al.*, 2000). As cell wall modifications, possibly leading to a restriction in cell growth, are well-known processes affected in plants exposed to Cd (Gutsch *et al*., 2018; Loix *et al*., 2017; Parrotta *et al*., 2015), the cell length reductions observed in our study might explain the differences with studies focusing on other stresses. At the lowest Cd exposure concentration, the reduction of the LER could even be fully explained by a shortening of mature cells. This suggests that leaf elongation at lower Cd concentrations is primarily impacted by a decrease in cell expansion rather than a decrease in cell production. However, l_{mat} is not significantly decreased further by the higher Cd level, indicating that there might be a minimum cell size for physiological functioning (Gazquez and Beemster, 2017).

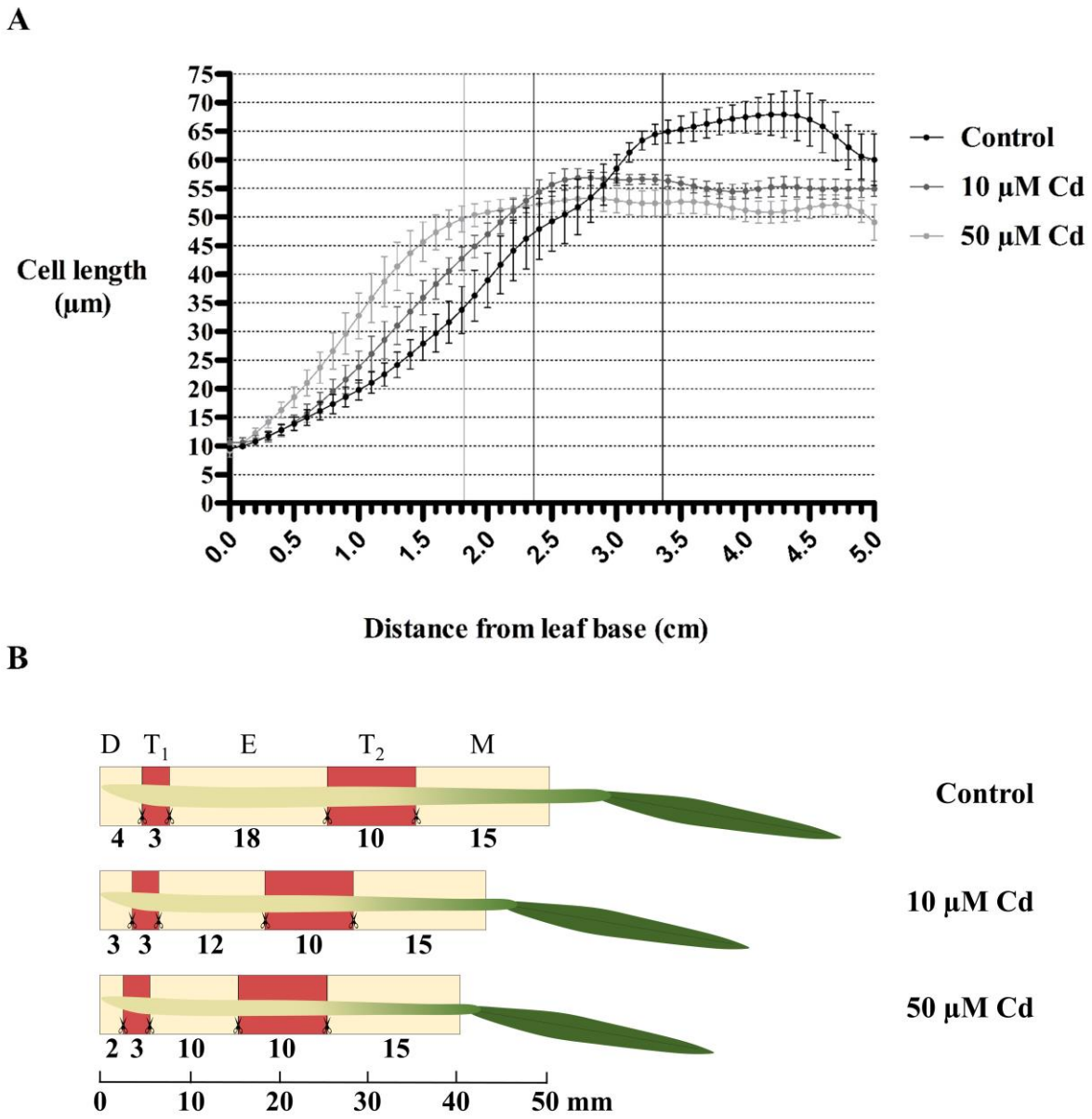

366

367 **Fig 3. The effect of Cd on the cell length profile along the growing rice leaf. A.** Leaf cell length
368 profile of the lower five centimeters of the sixth leaf of control and Cd-exposed plants. Values
369 represent the mean ± S.E. of 5 plants. Vertical lines indicate the end of the growth zone of the
370 respective conditions. **B.** Zone-specific sampling for Cd concentration and gene expression analysis
371 based on results of the cell length profile. Numbers under each segment indicate the exact size in
372 millimeters of that segment. Abbreviations; division zone (D), transition zone 1 (T_1), elongation zone
373 (E), transition zone 2 (T_2) and maturation zone (M).

The cell production was not significantly reduced for both Cd exposure conditions. This value is dependent on the number of cells located in the meristem and the average cell division rate. This last parameter was unaffected by Cd exposure. However, the division zone progressively contained significantly fewer cells with increasing Cd concentrations (Table 1). This last finding was a direct consequence of a smaller meristem size in Cd-exposed plants. Based on observations through DAPI staining, the division zone was reduced from 4.8 mm for control plants to 3.8 mm for the 10 µM Cd-exposed plants and 2.8 mm for the 50 µM Cd-exposed plants. Meristem size control was also suggested to be an important mechanism under drought stress in maize leaves (Avramova *et al.*, 2017). Adjustment to salt stress in *A. thaliana* roots was characterized by two phases; a rapid inhibition of the cell cycle followed by a decrease in meristem size but similar cell cycle durations (West *et al.*, 2004). A similar mechanism was seen in wheat leaves in response to soil compaction. The first leaves of plants grown under high soil resistance showed cells that were dividing slower, but leaves that appeared later had a reduced meristem size (Beemster et al., 1996). In our study, plants were exposed to Cd when the fourth leaf appeared, and kinematic analysis was performed on the sixth leaf, explaining why meristem size adjustment in this leaf might have already occurred.

Since the LER is clearly affected in Cd-exposed plants, these kinematic data provided a map of the growth zone on which spatial sampling of specific developmental stages of the growing tissues (proliferating, expanding, mature and the transitions between these main stages) is based. Figure 3B depicts the manner by which the growth zone is sampled for all conditions for gene expression analysis. Because the size of the meristem and growth zone is reduced in Cd-exposed plants, the individual segments were shortened, which enables comparison of the zones between the different conditions (Fig. 3B). In conclusion, the disturbance of developmental processes such as cell division and expansion by Cd could be coupled with molecular measurements by determination of the leaf growth zone (Sprangers *et al.*, 2016).

3.3. Flow cytometry as a valid method for mapping different growth zones under Cd stress

In order to study the cell cycle progression along the leaf axis, we performed flow cytometry. Rice vegetative tissue merely contains cells with a 2C or 4C ploidy level, because the process of endoreplication only occurs during seed endosperm development (Su'udi *et al.*, 2012). Nonetheless, flow cytometry can provide additional insights into the cell cycle progression in leaves of rice plants grown under different Cd exposure conditions. The obtained data show that at the base of the leaves up to 20% of cells have a 4C ploidy level. This fraction drops to a mere 2-3% around 2.5 cm from the base of control leaves and this occurs progressively closer to the base in Cd-exposed plants (Fig. 4A-C). The fraction of 4C cells is significantly lower in the second segment (between 0.5 and 1 cm from the base) for the 50 µM Cd-exposed plants. For the 10 µM Cd-exposed plants, this ratio is significantly lower than control plants at the third segment (between 1 and 1.5 cm from the base) (Fig. 4D). These results again display a clear Cd dose-dependent response of the leaf growth zone, which was also observed using the kinematic analysis, and thus confirm that the meristem size decreases with increasing Cd concentrations. However, flow cytometric analysis shows that the meristem possibly extends over the first 2 cm in control plants, which is much larger than what was assessed by DAPI staining (e.g. 4.8 mm for control plants). A possible explanation is that flow cytometric analysis encompasses whole tissue analysis, while DAPI staining is only based on cells in the adaxial epidermis. Indeed, in maize leaves, the mesophyll cells were shown to divide longer resulting in a division zone twice as long as the one of epidermal cells (Tardieu *et al.*, 2000). The results for the control plants in our study are in accordance with the ones obtained by Pettkó-Szandtner and colleagues (2015), who also observed a rapid decline in the 4C fraction after the first cm followed by a basal level of 4C cells in leaves of *O. sativa* L. cv. Nipponbare plants (Pettkó-Szandtner *et al.*, 2015).

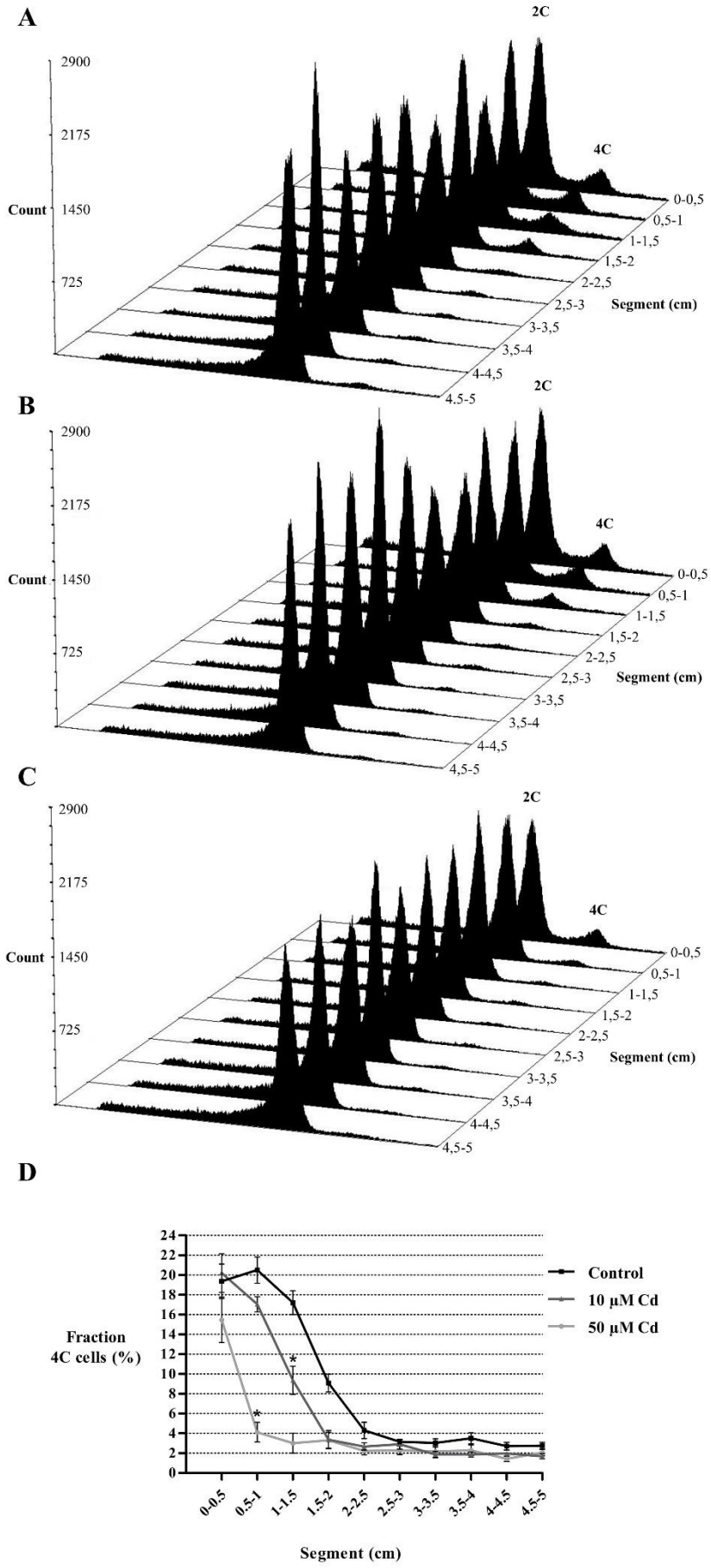
A
2C
4C
2900
2175
1450
725
Count
0-0,5
0,5-1
1-1,5
1,5-2
2-2,5
2,5-3
3-3,5
3,5-4
4-4,5
4,5-5
Segment (cm)
B
2C
4C
2900
2175
1450
725
Count
0-0,5
0,5-1
1-1,5
1,5-2
2-2,5
2,5-3
3-3,5
3,5-4
4-4,5
4,5-5
Segment (cm)
C
2C
4C
2900
2175
1450
725
Count
0-0,5
0,5-1
1-1,5
1,5-2
2-2,5
2,5-3
3-3,5
3,5-4
4-4,5
4,5-5
Segment (cm)
D
Fraction
4C cells (%)
24
22
20
18
16
14
12
10
8
6
4
2
0
Control
10 µM Cd
50 µM Cd
*
*
*
0-0.5
0.5-1
1-1.5
1.5-2
2-2.5
2.5-3
3-3.5
3.5-4
4-4.5
4.5-5
Segment (cm)

424

Fig. 4 Nuclear DNA content distribution along the leaf axis in response to Cd. **A-C.** Merged flow cytometry plots of at least 5 replicates for each segment and condition. Y-axis indicates the number of cells registered, X-axis represent the PI fluorescence intensity and Z-axis shows ten different segments (5 mm/segment) along the leaf base. **A.** Control plants. **B.** Plants exposed to 10 µM Cd. **C.** Plants exposed to 50 µM Cd. **D.** Fraction of 4C cells for each segment. Values represent the mean ± S.E. of 5 to 6 plants. Asterisk indicates a significant difference compared to the control within that segment (One-way ANOVA, p-value < 0.05).

3.4. Cadmium accumulates mainly within the leaf meristem and first transition zone

Both Cd-exposed conditions showed a similar pattern with the highest Cd accumulation in the division zone and the first transition zone followed by a significant drop in the elongation zone and onwards (Fig. 5). In a radioisotope-labeled tracer experiment where rice plants in hydroponic culture were fed with ^{107}Cd, the shoot base was the predominant place of Cd accumulation with only a limited amount of Cd present in the leaf sheath and no Cd in the blades after 36 h of feeding during the vegetative stage (Fujimaki *et al.*, 2010). In our study, the Cd concentration was determined in expanding leaves, which still lack a clear differentiation between leaf sheath and leaf blade. In mature leaves, Kobayashi and colleagues (2013) stated that the higher Cd accumulation in the leaf sheath compared to the leaf blade might be the result of a difference in complexation ability and/or ion selectivity of the tissue separating the two leaf parts. Since our results indicate that there is no clear difference in Cd accumulation between the elongation zone and the blade zone, these processes might therefore not be functional yet.

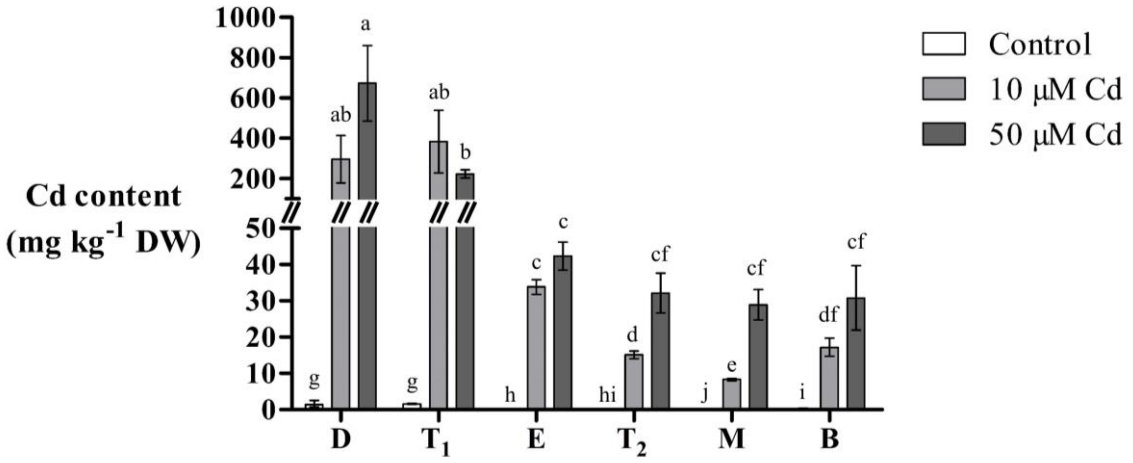

Fig. 5 Cadmium accumulation in different rice leaf zones. Bars show the mean ± SE of 4 biological replicates. Control bars for the E, T_2, M and B zone are not visible since the Cd concentration was less than 0.5 mg kg^{-1} DW. Abbreviations; division zone (D), transition zone 1 (T_1), elongation zone (E), transition zone 2 (T_2) and mature zone (M), blade (B).

3.5. Cell cycle progression genes are downregulated in Cd-exposed plants across the leaf growth zones.

To investigate the reduction of the LER and the smaller meristem size, the expression levels of four cell cycle genes were measured to test their response to 10 µM Cd exposure (Table 2). The *Retinoblastoma-related protein 2* (*RBR2*) gene was significantly down-regulated by Cd exposure across the whole leaf growth zone in our study based on the fold change expression levels. Furthermore, in accordance to Pettkó-Szandtner and colleagues (2015), this gene showed a constitutive expression when the different leaf zones were compared. Next, two cell cycle-stimulating genes were tested, namely *Cyclin-dependent kinase B1-1* (*CDKB1;1*) and *Cyclin-dependent kinase B2-1* (*CDKB2;1*). These kinases phosphorylate a range of substrates which are important in the G1/S and G2/M transitions, thereby stimulating the cell cycle (Inzé and De Veylder, 2006). Both genes were significantly downregulated across the growth zone under Cd exposure and they showed the highest expression levels in the D and T_1 zone, which emphasizes their role in the cell cycle. Lastly, a cyclin gene was tested, more specifically

Cyclin-A3-2 (*CYCA3;2*). Cyclin proteins typically activate CDKs, thereby forming the basic machinery for cell cycle progression (Pettkó-Szandtner *et al*., 2015). Whereas the expression level of *CYCA3;2* was the highest in the meristem and the lowest in the mature zone, its expression was unresponsive to Cd in our study.

Overall, these results show that cell cycle progression is negatively affected by Cd, as the expression level of cell cycle genes is downregulated across the whole growth zone. Although no significantly lower cell production rate was found for the 10 µM Cd-exposed plants in the kinematic analysis, the smaller meristem size correlates with the lower cell cycle genes expression levels. Moreover, the gene expression data are in accordance to the flow cytometric measurements, which demonstrated a lower amount of 4C cells within the third segment for the 10 µM Cd condition indicative of a lower number of dividing cells.

Table 2. Expression levels of the cell cycle genes *RBR2*, *CDKB1;1*, *CDKB2;1* and *CYCA3;2* under controlled and 10 µM Cd-exposed conditions. The first row of each gene represents the expression level in the different leaf growth zones expressed relative to the division zone of control plants (set at 1.00). The second row represents the fold change between the control and 10 µM Cd-exposed plants within that specific leaf zone. Asterisks indicate a significant downregulation under Cd exposure across all zones together based on the fold change (Two-way ANOVA; p-value < 0.05).

	LOCATION									
	D		**T_1**		**E**		**T_2**		**M**	
GENE	**Control**	**10 µM Cd**	**Control**	**10 µM Cd**	**Control**	**10 µM Cd**	**Control**	**10 µM Cd**	**Control**	**10 µM Cd**
RBR2*	1.00 ± 0.07	0.74 ± 0.04	1.64 ± 0.4	1.34 ± 0.21	0.95 ± 0.11	1.15 ± 0.14	1.57 ± 0.2	1.39 ± 0.07	1.46 ± 0.1	1.06 ± 0.03
	0.74 ± 0.04		0.82 ± 0.13		1.21 ± 0.14		0.89 ± 0.04		0.73 ± 0.02	
CDKB1;1*	1.00 ± 0.04	0.92 ± 0.13	1.13 ± 0.1	0.87 ± 0.01	0.65 ± 0.06	0.42 ± 0.14	0.13 ± 0.03	0.07 ± 0.01	0.04 ± 0.01	0.04 ± 0.01
	0.92 ± 0.13		0.77 ± 0.01		0.65 ± 0.21		0.51 ± 0.03		0.79 ± 0.09	
CDKB1;1*	1.00 ± 0.11	0.77 ± 0.13	0.91 ± 0.09	0.85 ± 0.09	0.48 ± 0.03	0.28 ± 0.1	0.03 ± 0.01	0.02 ± 0.01	0.01 ± 0.01	0.01 ± 0.01
	0.77 ± 0.13		0.93 ± 0.1		0.57 ± 0.2		0.49 ± 0.15		0.6 ± 0.16	
CYCA3;2	1.00 ± 0.07	0.94 ± 0.14	0.99 ± 0.01	0.93 ± 0.17	0.39 ± 0.03	0.37 ± 0.03	0.06 ± 0.01	0.07 ± 0.01	0.05 ± 0.01	0.04 ± 0.01
	0.94 ± 0.14		0.94 ± 0.17		0.95 ± 0.06		1.13 ± 0.13		0.96 ± 0.15	

3.6. Catalase and ascorbate peroxidase isoforms show leaf segment-specific responses to Cd

Cadmium is a known inducer of oxidative stress and its accumulation differs between leaf zones. Furthermore, several studies suggest that oxidative stress is involved in the inhibition of cell cycle progression, thereby reducing plant growth (Hendrix *et al.*, 2018; Huybrechts *et al.*, 2019). As it is relatively stable and able to cross cell membranes, H_2O_2 is particularly under attention as a signaling molecule (Mhamdi and Van Breusegem, 2018). Especially in the leaves, H_2O_2 was proven to be an important inducer of oxidative stress during Cd exposure (Smeets *et al.*, 2008). Considering the importance of H_2O_2, we investigated the gene expression levels of *SOD* isoforms (conversion of superoxide into H_2O_2 and O_2) and *CAT* and *APX* isoforms (H_2O_2 scavenging). While no leaf zone-specific responses were found for the *SOD* isoforms (Supplemental Table A3), *CAT* and *APX* isoforms differed greatly in abundance depending on the leaf zone and showed leaf zone specific upregulations under Cd exposure. Both CAT and APX scavenge H_2O_2, yet the affinities of both enzymes for H_2O_2 show great differences (CAT in the mM range and APX in the µM range). Therefore, CAT was proposed to serve the role of bulk H_2O_2 neutralization under stressful conditions, while APX might be involved in fine-tuning (Cuypers *et al.*, 2016; Mittler, 2002).

Rice has four *CAT* genes: *OsCATA, OsCATB, OsCATC* and *OsCATD,* which through alternative splicing encode for seven proteins located in the cytosol, peroxisomes and plasma membrane (Alam and Ghosh, 2018). The newest member, *OsCATD,* displays a low expression level throughout all developmental stages and tissues and was shown to be irresponsive to abiotic stress (Alam and Ghosh, 2018). Therefore, its specific function still has to be investigated. Structural and functional gene analysis indicate that *OsCATA* matches to the *A. thaliana AtCAT3, OsCATB* to *AtCAT1* and *OsCATC* to *AtCAT2* (Liu *et al.*, 2019; Mhamdi *et al.*, 2010). *OsCAT* transcript levels might vary spatially and temporally in plant

organs and respond differently under various environmental stresses (Du *et al.*, 2008; L. Hu *et al.*, 2016b; Iwamoto *et al.*, 2000).

Analysis of *CAT* isoform expression further reveals high variability along the leaf axis in control plants (Fig 6.). *OsCATA* expression was almost absent in the first two leaf growth zones, but became the dominant form in the elongation and mature zone, which might suggest an important role for *OsCATA* in maturing cells under controlled conditions. *OsCATB* showed a constitutive expression across all zones, while the relative abundance of *OsCATC* was almost negligible compared to the other two isoforms. These findings are consistent with earlier reports showing that *OsCATA* has the highest expression level in the leaf sheath, *OsCATB* in the roots of seedlings and *OsCATC* in the leaf blade (Iwamoto *et al.*, 2000). A similar expression for *OsCATA* and *OsCATC* was found in the blades and sheaths by Lin and colleagues (Lin *et al.*, 2012). Another study reported *OsCATA* expression to be five times higher than that of *OsCATC* in rice leaves (Hu *et al.*, 2017). The findings of our study suggest that even within the leaf growth zone very pronounced differences might occur in *OsCAT* expression.

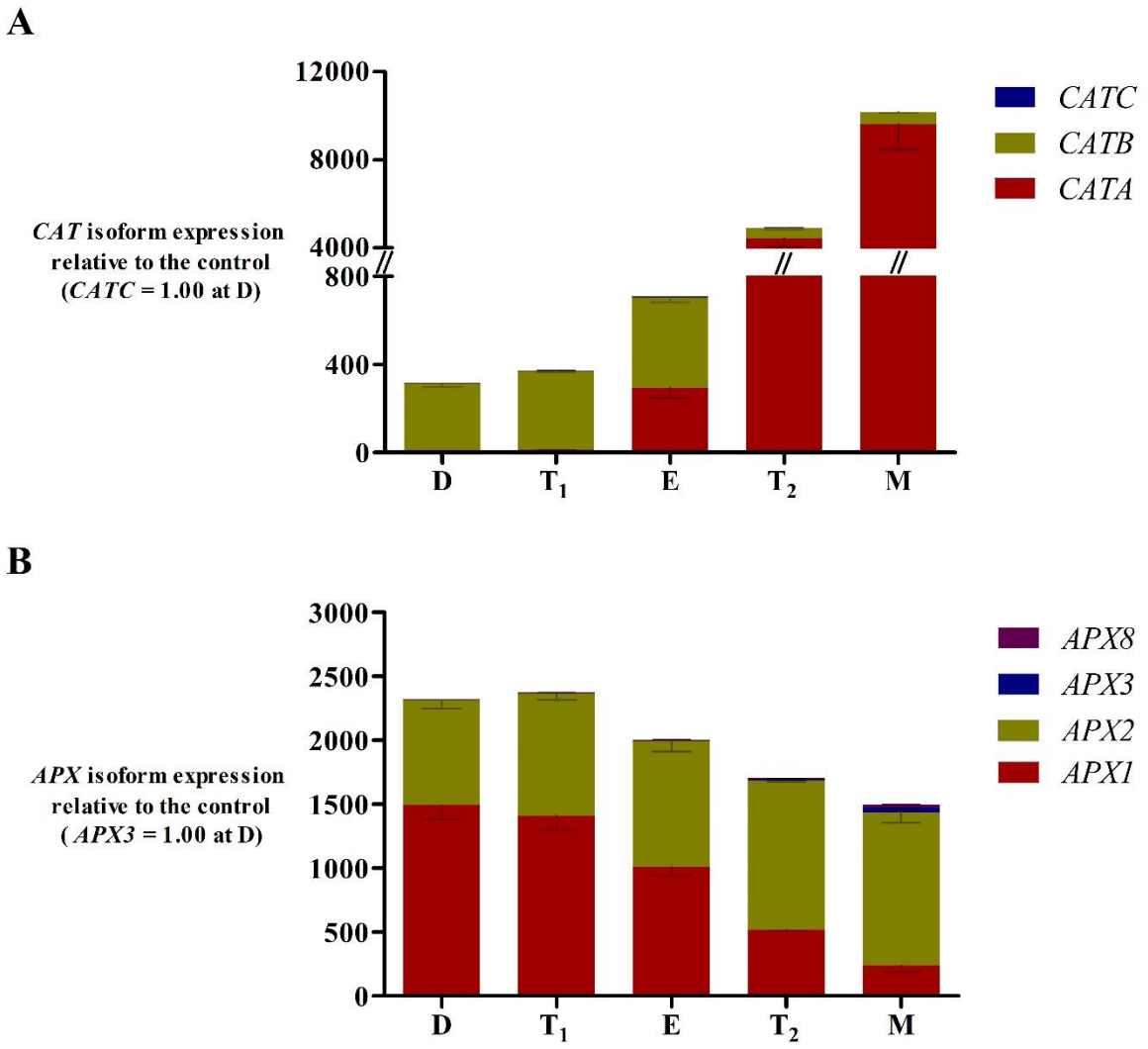

Fig 6. Catalase (**A**) and ascorbate peroxidase (**B**) isoform expression across different leaf growth zones. The value of the lowest abundant isoform in the division zone was set to 1.00 both for *CAT* and *APX*. All other isoforms in the different leaf growth zones were calculated relative to this value. Bars show the mean ± SE of 4 biological replicates. Standard errors on bars are only shown downwards.

In this study, *OsCATA, OsCATB and OsCATC* expression was analyzed in the leaf growth zone of control and Cd-exposed plants (Fig. 3B). *OsCATA* and *OsCATC* were both significantly upregulated across the growth zone in Cd-exposed plants (denoted by asterisk in Table 3). *CATA* additionally showed segment-specific upregulations in the first transition- and elongation zone. These two isoforms were also found to be the stress-responsive members

across a broad range of different biotic and abiotic stresses (Alam and Ghosh, 2018). In *A. thaliana*, *AtCAT1* and *AtCAT3* were upregulated after respectively 24 h and 48 h of Cd exposure, while *AtCAT2* was down-regulated after 24 h (Jozefczak *et al.*, 2014). CAT proteins in pea plants were proposed to be posttranslationally modified under Cd stress, since expression of *CAT* transcripts were upregulated but CAT activity was reduced (Romero-Puertas *et al.*, 2007). Smeets and colleagues also observed a transcriptional *AtCAT1* upregulation but no significant changes in CAT activities of Cd-exposed *A. thaliana* (Smeets *et al.*, 2008). To conclude, *CAT* isoforms are highly differentially expressed in distinct leaf growth zones under control conditions. While *CATA* was Cd-responsive in the first transition- and elongation zone, both *CATA* and *CATC* were significantly induced upon Cd-exposure in all zones together. To explain these results, more research is needed related to specific CAT activities and ROS fluxes within the leaf growth zone.

Table 3. Expression levels of catalase and ascorbate peroxidase isoforms at 10 µM Cd exposure in different leaf growth zones expressed relative to the same zone under control conditions (set at 1.00). Green color indicates significant Cd-induced upregulations (Two-way ANOVA; p-value < 0.05). Asterisks indicate a significant upregulation under Cd exposure in all zones together for that isoform.

	LOCATION				
GENE	**D**	**T_1**	**E**	**T_2**	**M**
*CATA**	3.85 ± 1.82	5.08 ± 1.00	6.11 ± 1.93	2.55 ± 0.31	0.97 ± 0.27
CATB	1.02 ± 0.07	0.99 ± 0.09	1.21 ± 0.18	1.02 ± 0.09	0.89 ± 0.05
*CATC**	2.44 ± 0.55	2 ± 0.23	1.59 ±0.23	1.07 ± 0.17	2.45 ± 1.02
APX1	0.99 ± 0.05	1.01 ± 0.06	1.18 ± 0.49	0.52 ± 0.05	0.73 ± 0.17
*APX2**	1.15 ± 0.06	1.17 ± 0.07	1.43 ± 0.11	1.09 ± 0.03	1.19 ± 0.09
*APX3**	0.98 ± 0.05	1.51 ± 0.17	1.37 ± 0.38	3.03 ± 0.22	0.9 ± 0.28
*APX8**	0.93 ± 0.07	0.9 ± 0.04	1.34 ± 0.15	2.84 ± 0.08	2.27 ± 0.83

In contrast to CAT, APX proteins make use of ascorbate as an electron donor to detoxify high levels of H_2O_2 (Cuypers *et al.*, 2016). In rice, eight *OsAPX* isoforms have been identified; two cytosolic forms (*OsAPX1* and *OsAPX2*), two located in the peroxisomes (*OsAPX3* and *OsAPX4*), three in the chloroplasts (*OsAPX5*, *OsAPX6* and *OsAPX7*), where *OsAPX6* fused with a green fluorescent protein was also found to be present in the mitochondria of transformed BY-2 tobacco cells, and one thylakoid-bound form (*OsAPX8*) (Teixeira *et al.*, 2006, 2004). Gene expression analysis of emerging rice seedlings displays specific patterns for each transcript. *OsAPX1* preferably accumulates in the roots, while *OsAPX2* is both present in the roots and shoot. *OsAPX3* and *OsAPX8* are exclusively present in the shoot (Teixeira *et al.*, 2006). Our study shows that in the meristematic leaf zone, *OsAPX1* was expressed at higher levels than *OsAPX2*, but dropped further away from the leaf base (Fig 6). Furthermore, *OsAPX3* and *OsAPX8* were almost absent until the second transition zone. This coincides with reaching the mature cell length and probably early chloroplast differentiation leading to APX accumulation in the thylakoid membrane.

OsAPX2, *OsAPX3* and *OsAPX8* showed an overall upregulation in response to Cd exposure (Table 3). Further segment-specific increases were observed in the elongation zone for *OsAPX2* and in the second transition zone for *OsAPX3* and *OsAPX8*. *OsAPX2* displays high similarity with the *AtAPX1*, which was proposed to be a central component in the ROS gene network in *A. thaliana* and showed cross-compartment protection during light stress (Davletova *et al.*, 2005; Li *et al.*, 2015). *Arabidopsis thaliana* plants also displayed an increase of *AtAPX2* in both roots and leaves after 24 h of Cd exposure (Jozefczak *et al.*, 2014). Under salt stress, *OsAPX2* was upregulated after 24 h, whereas *OsAPX8* showed a rapid downregulation followed by a recovery to half its initial expression (Teixeira *et al.*, 2006). Exogenous treatment of rice leaves with H_2O_2 led to an increase of *OsAPX1* and *OsAPX2* transcripts, but *OsAPX8* was again rapidly downregulated. This finding indicates an

important role in chloroplast redox protection during early leaf senescence for *OsAPX8* (Li *et al.*, 2015). Under well-watered conditions, *apx8* deficient mutants displayed an induction of compensating redox regulating mechanisms, suggesting a signaling role for *OsAPX8* through H_2O_2 homeostasis (Cunha *et al.*, 2019). In another study, Cd exposure for 3 days led instead to a decrease in *OsAPX1*, *OsAPX2* and *OsAPX3* in rice leaves (Hu *et al.*, 2017). This contradicts with our findings. However, one should be careful when comparing these results. At time of appearance of the sixth leaf, our plants were already exposed to Cd for minimum one week longer than the plants in the study by Hu and colleagues (2017). Moreover, our results indicate that the leaf growth zone is already highly variable considering both *CAT* and *APX* gene expression, thus observed differences with whole leaf sampling might not be comparable. Moreover, in maize plants, CAT and APX activity where both highest in the proliferating tissues at the base of the leaf and upregulated by drought stress (Avramova *et al.*, 2017).

While CAT functions as the major scavenging protein to remove excess H_2O_2 during stress situations, APX was proposed to serve as a H_2O_2 fine-tuning mechanism, which could be important in secondary cell wall depositions in *A. thaliana* (Shafi *et al.*, 2015). Consistently, in the Cd-exposed plants, the mature cell length was much smaller, suggesting possible limitations on cell size through the cell wall formation. This correlates with an upregulation of different *APX* isoforms in this zone and suggests a possible role in secondary cell wall biosynthesis upon Cd exposure.

4. Conclusion and future perspectives

This study shows the negative effects of Cd on the leaf growth of *O. sativa* L. cv. Nipponbare. Kinematic analysis revealed a shortening of the meristem and elongation zone in Cd-exposed plants, resulting in a reduced FLL. Flow cytometric measurements yielded results that were in

the same line, although the size of the meristem was larger for all conditions. Three out of four analyzed cell cycle genes showed a lower expression level in the leaf growth zone of Cd-exposed plants, which is in agreement with the reduction of leaf growth. The gene expression analysis of *CAT* and *APX* genes revealed specific expression patterns across the leaf growth zone, suggesting oxidative stress levels might be differently regulated depending on the observed zone. Therefore, future measurements of H_2O_2 levels, enzymatic activities of CAT and APX and other antioxidant defense mechanisms in these zones would be interesting. In conclusion, this study shows that high-resolution sampling could be an important tool for future research, as the effect of Cd on cell division, cell expansion and mature cells can be analyzed separately.

Author contributions

All authors participated in the conception of the topic. M.H. and A.C. wrote the manuscript. M.H. made the figures and tables. S.H. and J.B. helped with the optimization of the experiments. All authors read and approved the final manuscript after critically revising it for important intellectual content.

Declarations of interest

The authors declare no conflict of interest.

Funding

Funding: This work was supported by the Research Foundation Flanders (FWO) by project funding for MH [G0B6716], SH [G0C7518CUY] and JB [G0B6716].

Acknowledgements

We thank the United States Department of Agriculture for kindly providing the Nipponbare rice seeds (GSOR-100). Additionally, we like to thank Ann Wijgaerts, Carine Put and Elsy Thijssen for their assistance in the lab.

References

Ahmad, P., Nabi, G., Ashraf, M., 2011. Cadmium-induced oxidative damage in mustard [Brassica juncea (L .) Czern . & Coss .] plants can be alleviated by salicylic acid. South African J. Bot. 77, 36–44. https://doi.org/10.1016/j.sajb.2010.05.003

Alam, N.B., Ghosh, A., 2018. Comprehensive analysis and transcript profi ling of Arabidopsis thaliana and Oryza sativa catalase gene family suggests their specific roles in development and stress responses. Plant Physiol. Biochem. 123, 54–64. https://doi.org/10.1016/j.plaphy.2017.11.018

Andriankaja, M., Dhondt, S., De Bodt, S., Vanhaeren, H., Coppens, F., De Milde, L., Mühlenbock, P., Skirycz, A., Gonzalez, N., Beemster, G.T.S., Inzé, D., 2012. Exit from Proliferation during Leaf Development in Arabidopsis thaliana : A Not-So-Gradual Process. Dev. Cell 22, 64–78. https://doi.org/10.1016/j.devcel.2011.11.011

Avramova, V., Abdelgawad, H., Vasileva, I., Petrova, A.S., Holek, A., Mariën, J., Asard, H., Beemster, G.T.S., 2017. High Antioxidant Activity Facilitates Maintenance of Cell Division in Leaves of Drought Tolerant Maize Hybrids. Front. Plant Sci. 8, 84. https://doi.org/10.3389/fpls.2017.00084

Avramova, V., Abdelgawad, H., Zhang, Z., Fotschki, B., Casadevall, R., Vergauwen, L., Knapen, D., Taleisnik, E., Guisez, Y., Asard, H., Beemster, G.T.S., 2015a. Drought Induces Distinct Growth Response, Protection, and Recovery Mechanisms in the Maize. Plant Physiol. 169, 1382–1396. https://doi.org/10.1104/pp.15.00276

Avramova, V., Sprangers, K., Beemster, G.T.S., 2015b. The Maize Leaf: Another Perspective on Growth Regulation. Trends Plant Sci. 20, 787–797. https://doi.org/10.1016/j.tplants.2015.09.002

Barroco, R.M., Peres, A., Droual, A., Veylder, L. De, Nguyen, L.S.L., Wolf, J. De, Mironov, V., Peerbolte, R., Beemster, G.T.S., Inzé, D., Broekaert, W.F., Frankard, V., 2006. The Cyclin-Dependent Kinase Inhibitor

642 Orysa; KRP1 Plays an Important Role in Seed Development of Rice. Plant Physiol. 142, 1053–1064.
643 https://doi.org/10.1104/pp.106.087056

644 Beemster, G.T.S., Masle, J., 1996. Effects of soil resistance to root penetration on leaf expansion in wheat (
645 Triticum aestivum L .): composition , number and size of epidermal cells in mature blades. J. Exp. Bot. 47,
646 1651-1662. https:// doi.org/10.1093/jxb/47.11.1651

647 Beemster, G.T.S., Masle, J., Williamson, R.E., Graham, D., 1996. Effects of soil resistance to root penetration on
648 leaf expansion in wheat (Triticum aestivum L.): kinematic analysis of leaf elongation. J. Exp. Bot. 47,
649 1663–1678. https://doi.org/10.1093/jxb/47.11.1663

650 Bustin, S.A., Benes, V., Garson, J.A., Hellemans, J., Huggett, J., Kubista, M., Mueller, R., Nolan, T., Pfaffl,
651 M.W., Shipley, G.L., Vandesompele, J., Wittwer CT., 2009. The MIQE Guidelines : Minimum
652 Information for Publication of Q uantitative Real-Time PCR Experiments. Clin. Chem. 55, 611–622.
653 https://doi.org/10.1373/clinchem.2008.112797

654 Clemens, S., Ma, J.F., 2016. Toxic Heavy Metal and Metalloid Accumulation in Crop Plants and Foods. Annu.
655 Rev. Plant Biol. 67, 489–512. https://doi.org/10.1146/annurev-arplant-043015-112301

656 Cunha, J.R., Carvalho, F.E.L., Lima-neto, M.C., Jardim-messeder, D., Cerqueira, J.V.A., Martins, M.O.,
657 Fontenele, A. V, Márgis-pinheiro, M., Komatsu, S., Silveira, J.A.G., 2019. Proteomic and physiological
658 approaches reveal new insights for uncover the role of rice thylakoidal APX in response to drought stress.
659 J. Proteomics 192, 125–136. https://doi.org/10.1016/j.jprot.2018.08.014

660 Cuypers, A., Hendrix, S., Amaral Dos Reis, R., De Smet, S., Deckers, J., Gielen, H., Jozefczak, M., Loix, C.,
661 Vercampt, H., Vangronsveld, J., Keunen, E., 2016. Hydrogen peroxide, signaling in disguise during metal
662 phytotoxicity. Front. Plant Sci. 7, 46. https://doi.org/10.3389/fpls.2016.00470

663 Cuypers, A., Plusquin, M., Remans, T., Jozefczak, M., Keunen, E., Gielen, H., Opdenakker, K., Nair, A.R.,
664 Munters, E., Artois, T.J., Nawrot, T., Vangronsveld, J., Smeets, K., Keunen, E., Gielen, H., Opdenakker,
665 K., Nair, A.R., Munters, E., Artois, T.J., Nawrot, T., Vangronsveld, J., Smeets, K., 2010. Cadmium stress:
666 An oxidative challenge. BioMetals 23, 927–940. https://doi.org/10.1007/s10534-010-9329-x

667 Cuypers, A., Smeets, K., Vangronsveld, J., 2009. Heavy Metal Stress in Plants, in: Plant Stress Biology. pp.

161–178.

Davletova, S., Rizhsky, L., Liang, H., Shengqiang, Z., Oliver, D.J., Coutu, J., Shulaev, V., Schlauch, K., Mittler, R., 2005. Cytosolic Ascorbate Peroxidase 1 Is a Central Component of the Reactive Oxygen Gene Network of Arabidopsis. Plant Cell 17, 268–281. https://doi.org/10.1105/tpc.104.026971.1

Du, Y., Wang, P., Chen, J., Song, C., 2008. Comprehensive Functional Analysis of the Catalase Gene Family in Arabidopsis thaliana. J. Integr. Plant Biol. 50, 1318–1326. https://doi.org/10.1111/j.1744-7909.2008.00741.x

Duan, Q., Lee, J., Liu, Y., Chen, H., Hu, H., 2016. Distribution of Heavy Metal Pollution in Surface Soil Samples in China: A Graphical Review. Bull. Environ. Contam. Toxicol. 97, 303–309. https://doi.org/10.1007/s00128-016-1857-9

Fina, J., Casadevall, R., Abdelgawad, H., Prinsen, E., Markakis, M.N., Beemster, G.T.S., Casati, P., 2017. UV-B Inhibits Leaf Growth through Changes in Growth Regulating Factors and Gibberellin Levels. Plant Physiol. 174, 1110–1126. https://doi.org/10.1104/pp.17.00365

Fiorani, F., Beemster, G.T.S., 2006. Quantitative analyses of cell division in plants. Plant Mol. Biol. 60, 963–979. https://doi.org/10.1007/s11103-005-4065-2

Fournier, C., Durand, J., Ljutovac, S., Schäufele, R., Gastal, F., Andrieu, B., 2005. A functional – structural model of elongation of the grass leaf and its relationships with the phyllochron. New Phytol. 166, 881–894. https://doi.org/10.1111/j.1469-8137.2005.01371.x

Fujimaki, S., Suzui, N., Ishioka, N.S., Kawachi, N., Ito, S., Chino, M., Nakamura, S. ichi, 2010. Tracing cadmium from culture to spikelet: noninvasive imaging and quantitative characterization of absorption, transport, and accumulation of cadmium in an intact rice plant. Plant Physiol. 152, 1796–1806. https://doi.org/10.1104/pp.109.151035

Gazquez, A., Beemster, G.T.S., 2017. What determines organ size differences between species? A meta-analysis of the cellular basis. New Phytol. 215, 299–308. https://doi.org/10.1111/nph.14573

Gazquez, A., Maiale, S.J., Rachoski, M.M., Vidal, A., Ruiz, O.A., Menéndez, A.B., Rodriguez, A.A., 2015. Physiological Response of Multiple Contrasting Rice (Oryza sativa L.) Cultivars to Suboptimal

694 Temperatures. J. Agron. Crop Sci. 201, 117–127. https://doi.org/10.1111/jac.12095

695 Gutsch, A., Keunen, E., Guerriero, G., Renaut, J., Cuypers, A., Hausman, J.F., Sergeant, K., 2018. Long-term
696 cadmium exposure influences the abundance of proteins that impact the cell wall structure in Medicago
697 sativa stems. Plant Biol. 20, 1023–1035. https://doi.org/10.1111/plb.12865

698 Hendrix, S., Keunen, E., Mertens, A.I.G., Beemster, G.T.S., Vangronsveld, J., Cuypers, A., 2018. Cell cycle
699 regulation in different leaves of Arabidopsis thaliana plants grown under control and cadmium-exposed
700 conditions. Environ. Exp. Bot. 155, 441–452. https://doi.org/10.1016/j.envexpbot.2018.06.026

701 Hu, L., Yang, Y., Jiang, L., Liu, S., 2016b. The catalase gene family in cucumber: genome-wide identification
702 and organization. Genet. Mol. Biol. 39, 408–415. https://doi.org/10.1590/1678-4685-GMB-2015-0192

703 Hu, S., Yu, Y., Chen, Q., Mu, G., Shen, Z., Zheng, L., 2017. OsMYB45 plays an important role in rice resistance
704 to cadmium stress. Plant Sci. 264, 1–8. https://doi.org/10.1016/j.plantsci.2017.08.002

705 Hu, Y., Cheng, H., Tao, S., 2016a. The Challenges and Solutions for Cadmium-contaminated Rice in China: A
706 Critical Review. Environ. Int. 92–93, 515–532. https://doi.org/10.1016/j.envint.2016.04.042

707 Huybrechts, M., Cuypers, A., Deckers, J., Iven, V., Vandionant, S., Jozefczak, M., Hendrix, S., 2019. Cadmium
708 and Plant Development: An Agony from Seed to Seed. Int. J. Mol. Sci. 20, 3971.
709 https://doi.org/10.3390/ijms20163971

710 Inzé, D., De Veylder, L., 2006. Cell Cycle Regulation in Plant Development. Annu. Rev. Genet. 40, 77–105.
711 https://doi.org/10.1146/annurev.genet.40.110405.090431

712 Iwamoto, M., Higo, H., Higo, K., 2000. Differential diurnal expression of rice catalase genes : the 5'-flanking
713 region of CatA is not sufficient for circadian control. Plant Sci. 151, 39–46. https://doi.org/10.1016/S0168-
714 9452(99)00194-6

715 Ji, Y., Tu, P., Wang, K., Gao, F., Yang, W., Zhu, Y., Li, S., 2014. Defining reference genes for quantitative real-
716 time PCR analysis of anther development in rice. Acta Biochimica et Biophysica Sinica 46, 305–312.
717 https://doi.org/10.1093/abbs/gmu002

718 Jozefczak, M., Keunen, E., Schat, H., Bliek, M., Hernández, L.E., Carleer, R., Remans, T., Bohler, S.,

719 Vangronsveld, J., Cuypers, A., 2014. Differential response of Arabidopsis leaves and roots to cadmium:
720 Glutathione-related chelating capacity vs antioxidant capacity. Plant Physiol. Biochem. 83, 1–9.
721 https://doi.org/10.1016/j.plaphy.2014.07.001

722 Kabata-Pendias, A., Pendias, H., 2001. Trace elements in soils and plants, 3rd ed, CRC Press. Boca Raton, USA.
723 https://doi.org/10.1201/b10158-25

724 Keunen, E., Truyens, S., Bruckers, L., Remans, T., Vangronsveld, J., Cuypers, A., 2011. Survival of Cd-exposed
725 Arabidopsis thaliana: Are these plants reproductively challenged? Plant Physiol. Biochem. 49, 1084–1091.
726 https://doi.org/10.1016/j.plaphy.2011.07.013

727 Li, Z., Su, D., Lei, B., Wang, F., Geng, W., Pan, G., Cheng, F., 2015. Transcriptional profile of genes involved
728 in ascorbate glutathione cycle in senescing leaves for an early senescence leaf (esl) rice mutant. J. Plant
729 Physiol. 176, 1–15. https://doi.org/10.1016/j.jplph.2014.09.020

730 Lin, A.H., Wang, Y.Q., Tang, J.Y., Xue, P., Li, C.L., Liu, L., Hu, B., Yang, F.Q., Loake, G.J., Chu, C.C., 2012.
731 Nitric Oxide and Protein S-Nitrosylation Are Integral to Hydrogen Peroxide-Induced Leaf Cell Death in
732 Rice. Plant Physiol. 158, 451–464. https://doi.org/10.1104/pp.111.184531

733 Liu, J., Cui, L., Xie, Z., Zhang, Z., Liu, E., Peng, X., 2019. Two NCA1 isoforms interact with catalase in a
734 mutually exclusive manner to redundantly regulate its activity in rice. BMC Plant Biol. 19, 1–10.
735 https://doi.org/10.1186/s12870-019-1707-0

736 Loix, C., Huybrechts, M., Vangronsveld, J., Gielen, M., Keunen, E., 2017. Reciprocal Interactions between
737 Cadmium-Induced Cell Wall Responses and Oxidative Stress in Plants. Front. Plant Sci. 8, 1867.
738 https://doi.org/10.3389/fpls.2017.01867

739 Lu, D., Wang, T., Persson, S., Mueller-Roeber, B., Schippers, J.H.M., 2014. Transcriptional control of ROS
740 homeostasis by KUODA1 regulates cell expansion during leaf development. Nat. Commun. 5, 3767.
741 https://doi.org/10.1038/ncomms4767

742 Mhamdi, A., Queval, G., Chaouch, S., Vanderauwera, S., Van Breusegem, F., Noctor, G., 2010. Catalase
743 function in plants : a focus on Arabidopsis mutants as stress-mimic models. J. Exp. Bot. 61, 4197–4220.
744 https://doi.org/10.1093/jxb/erq282

Mhamdi, A., Van Breusegem, F., 2018. Reactive oxygen species in plant development. Development 145. https://doi.org/10.1242/dev.164376

Mittler, R., 2017. ROS Are Good. Trends Plant Sci. 22, 11–19. https://doi.org/10.1016/j.tplants.2016.08.002

Mittler, R., 2002. Oxidative stress, antioxidants and stress tolerance. Trends Plant Sci. 7, 405–410. https://doi.org/10.1016/S1360-1385(02)02312-9

Müller, K., Linkies, A., Vreeburg, R.A., Fry, S.C., Krieger-Liszkay, A., Leubner-Metzger, G., 2009. In Vivo Cell Wall Loosening by Hydroxyl Radicals during Cress Seed Germination and Elongation Growth. Plant Physiol. 150, 1855–1865. https://doi.org/10.1104/pp.109.139204

Nelissen, H., Sun, X.H., Rymen, B., Jikumaru, Y., Kojima, M., Takebayashi, Y., Abbeloos, R., Demuynck, K., Storme, V., Vuylsteke, M., Block, J. De, Herman, D., Coppens, F., Maere, S., Kamiya, Y., Sakakibara, H., Beemster, G.T.S., Inzé, D., 2018. The reduction in maize leaf growth under mild drought affects the transition between cell division and cell expansion and cannot be restored by elevated gibberellic acid levels. Plant Biotechnol. J. 16, 615–627. https://doi.org/10.1111/pbi.12801

Parent, B., Conejero, G., Tardieu, F., 2009. Spatial and temporal analysis of non-steady elongation of rice leaves. Plant, Cell Environ. 32, 1561–1572. https://doi.org/10.1111/j.1365-3040.2009.02020.x

Parrotta, L., Guerriero, G., Sergeant, K., Cai, G., Hausman, J.-F., 2015. Target or barrier? The cell wall of early- and later-diverging plants vs cadmium toxicity: differences in the response mechanisms. Front. Plant Sci. 6, 133. https://doi.org/10.3389/fpls.2015.00133

Pettkó-Szandtner, A., Cserháti, M., Barrôco, R.M., Hariharan, S., Dudits, D., Beemster, G.T.S., 2015. Core cell cycle regulatory genes in rice and their expression profiles across the growth zone of the leaf. J. Plant Res. 128, 953–974. https://doi.org/10.1007/s10265-015-0754-3

R Core Team, 2014. R: A language and environment for statistical computing. R Foundation for Statistical Computing, Vienna, Austria. http://www.R-project.org/

Remans, T., Keunen, E., Bex, G.J., Smeets, K., Vangronsveld, J., Cuypers, A., 2014. Reliable Gene Expression Analysis by Reverse Transcription- Quantitative PCR: Reporting and Minimizing the Uncertainty in Data Accuracy. Plant Cell 26, 3829–3837. https://doi.org/10.1105/tpc.114.130641

771 Rizwan, M., Ali, S., Adrees, M., Ibrahim, M., Tsang, D.C.W., Zia-ur-rehman, M., Zahir, Z.A., Rinklebe, J.,
772 Tack, F.M.G., Ok, Y.S., 2017. A critical review on effects, tolerance mechanisms and management of
773 cadmium in vegetables. Chemosphere 182, 90–105. https://doi.org/10.1016/j.chemosphere.2017.05.013

774 Rizwan, M., Ali, S., Adrees, M., Rizvi, H., Zia-ur-rehman, M., Hannan, F., Qayyum, M.F., Hafeez, F., Ok, Y.S.,
775 2016. Cadmium stress in rice: toxic effects, tolerance mechanisms, and management: a critical review.
776 Environ. Sci. Pollut. Res. 23, 17859–17879. https://doi.org/10.1007/s11356-016-6436-4

777 Romero-Puertas, M.C., Corpas, F.J., Rodriguez-Serrano, M., Gómez, M., del Río, L.A., Sandalio, L.M., 2007.
778 Differential expression and regulation of antioxidative enzymes by cadmium in pea plants. J. Plant
779 Physiol. 164, 1346–1357. https://doi.org/10.1016/j.jplph.2006.06.018

780 Rymen, B., Fiorani, F., Kartal, F., Vandepoele, K., Inzé, D., Beemster, G.T.S., 2007. Cold Nights Impair Leaf
781 Growth and Cell Cycle Progression in Maize through Transcriptional Changes of Cell Cycle genes. Plant
782 Physiol. 143, 1429–1438. https://doi.org/10.1104/pp.106.093948

783 Saidi, I., Chtourou, Y., Djebali, W., 2014. Selenium alleviates cadmium toxicity by preventing oxidative stress in
784 sunflower (Helianthus annuus) seedlings. J. Plant Physiol. 171, 85–91.
785 https://doi.org/10.1016/j.jplph.2013.09.024

786 Sandalio, L.M., Dalurzo, H.C., Gómez, M., Romero-Puertas, M.C., del Río, L.A., 2001. Cadmium-induced
787 changes in the growth and oxidative metabolism of pea plants. J. Exp. Bot. 52, 2115–2126.

788 Schippers, J.H.M., Foyer, C.H., Dongen, J.T. Van, 2016. Redox regulation in shoot growth, SAM maintenance
789 and flowering. Curr. Opin. Plant Biol. 29, 121–128. https://doi.org/10.1016/j.pbi.2015.11.009

790 Schmidt, R., Kunkowska, A.B., Schippers, J.H.M., 2016. Role of Reactive Oxygen Species during Cell
791 Expansion in Leaves. Plant Physiol. 172, 2098–2106. https://doi.org/10.1104/pp.16.00426

792 Schneider, C.A., Rasband, W.S., Eliceiri, K.W, 2012. NIH Image to ImageJ: 25 years of image analysis. Nature
793 Methods 9, 671-675. https://doi.org/10.1038/nmeth.2089

794 Schopfer, P., 1996. Hydrogen peroxide-mediated cell-wall stiffening in vitro in maize coleoptiles. Planta 199,
795 43–49. https://doi.org/10.1007/BF00196879

796 Shafi, A., Chauhan, R., Gill, T., Swarnkar, M.K., Sreenivasulu, Y., Kumar, S., Kumar, N., Shankar, R., Ahuja,
797 P.S., Singh, A.K., 2015. Expression of SOD and APX genes positively regulates secondary cell wall
798 biosynthesis and promotes plant growth and yield in Arabidopsis under salt stress. Plant Mol. Biol. 87,
799 615–631. https://doi.org/10.1007/s11103-015-0301-6

800 Smeets, K., Ruytinx, J., Semane, B., Van Belleghem, F., Remans, T., Van Sanden, S., Vangronsveld, J.,
801 Cuypers, A., 2008. Cadmium-induced transcriptional and enzymatic alterations related to oxidative stress.
802 Environ. Exp. Bot. 63, 1–8. https://doi.org/10.1016/j.envexpbot.2007.10.028

803 Smeets, K, Ruytinx, J., Van Belleghem, F., Semane, B., Lin, D., Vangronsveld, J., Cuypers, A., 2008. Critical
804 evaluation and statistical validation of a hydroponic culture system for Arabidopsis thaliana. Plant Physiol
805 Biochem 46, 212–218. https://doi.org/10.1016/j.plaphy.2007.09.014

806 Sobkowiak, R., Deckert, J., 2003. Cadmium-induced changes in growth and cell cycle gene expression in
807 suspension-culture cells of soybean. Plant Physiol. Biochem. 41, 767–772. https://doi.org/10.1016/S0981-
808 9428(03)00101-3

809 Sprangers, K., Avramova, V., Beemster, G.T.S., 2016. Kinematic Analysis of Cell Division and Expansion:
810 Quantifying the Cellular Basis of Growth and Sampling Developmental Zones in Zea mays
811 Leaves. J. Vis. Exp. 118, 54887. https://doi.org/10.3791/54887

812 Su'udi, M., Cha, J., Jung, M.H., Ermawati, N., Han, C.D., Kim, M.G., Woo, Y.M., Son, D., 2012. Potential role
813 of the rice OsCCS52A gene in endoreduplication. Planta 235, 387–397. https://doi.org/10.1007/s00425-
814 011-1515-8

815 Tardieu, F., Reymond, M., Hamard, P., Granier, C., Muller, B., 2000. Spatial distributions of expansion rate, cell
816 division rate and cell size in maize leaves: a synthesis of the effects of soil water status, evaporative
817 demand and temperature. J. Exp. Bot. 51, 1505–1514. https://doi.org/10.1093/jexbot/51.350.1505

818 Teixeira, F.K., Menezes-Benavente, L., Galvão, V.C., Margis, R., Margis-Pinheiro, M., 2006. Rice ascorbate
819 peroxidase gene family encodes functionally diverse isoforms localized in different subcellular
820 compartments. Planta 224, 300–314. https://doi.org/10.1007/s00425-005-0214-8

821 Teixeira, F.K., Menezes-benavente, L., Margis, R., Margis-Pinheiro, M., 2004. Analysis of the Molecular

Evolutionary History of the Ascorbate Peroxidase Gene Family: Inferences from the Rice Genome. J. Mol. Evol. 59, 761–770. https://doi.org/10.1007/s00239-004-2666-z

Tsukagoshi, H., 2012. Defective root growth triggered by oxidative stress is controlled through the expression of cell cycle-related genes. Plant Sci. 197, 30–39. https://doi.org/10.1016/j.plantsci.2012.08.011

Tsukagoshi, H., Busch, W., Benfey, P.N., 2010. Transcriptional Regulation of ROS Controls Transition from Proliferation to Differentiation in the Root. Cell 143, 606–616. https://doi.org/10.1016/j.cell.2010.10.020

Valledor, L., Escandon, M., Meijon, M., Nukarinen, E., Canal, M.J., Wolfram, W., 2014. A universal protocol for the combined isolation of metabolites, DNA, long RNAs, small RNAs, and proteins from plants and microorganisms. Plant J. 79, 173–180. https://doi.org/10.1111/tpj.12546

Wand M.P., Jones M.C.,1995. Kernel Smoothing. Chapman and Hall, London

West, G., Inzé, D., Beemster, G.T.S., 2004. Cell Cycle Modulation in the Response of the Primary Root of Arabidopsis to Salt Stress. Plant Physiol. 135, 1050–1058. https://doi.org/10.1104/pp.104.040022.termining

Yeo, A.R., Lee, K.S., Izard, P., Boursier, P.J., Flowers, T.J., 1991. Short- and Long-Term Effects of Salinity on Leaf Growth in Rice (Oryza sativa L.). J. Exp. Bot. 42, 881–889. https://doi.org/10.1093/jxb/42.7.881

Yoshida, S., Forno, D.A., Cock, J.H., Gomez, K.A., 1971. Laboratory Manual for Physiological Studies of Rice. https://doi.org/10.1017/CBO9781107415324.004

Zhao, F.Y., Wang, K., Zhang, S.Y., Ren, J., Liu, T., Wang, X., 2014. Crosstalk between ABA, auxin, MAPK signaling, and the cell cycle in cadmium-stressed rice seedlings. Acta Physiol. Plant. 36, 1879–1892. https://doi.org/10.1007/s11738-014-1564-2

Supplemental material

Table A1. Overview of reference genes and genes of interest used for gene expression analysis. A primer concentration of 300nM was used. E-E-jn: exon-exon junction; UTR: untranslated region

Gene	Locus	Forward primer (5'-3')	Reverse primer (5'-3')	Exon location	Amplicon size	Reference
eIF4A-3	*Os01g45190*	ATCCAGTTCGGATCCTTGTG	TGCAGAAAATGACAGCTTGG	Exon 4 and Exon 5	150	Ji et al., 2014
UPF3	*Os04g35920*	TTCTGTCAGCAAGCAGATGG	GTTGGCAGAGGCTCTCTTTG	Exon 9 and Exon 10	189	Ji et al., 2014
eEF-1α	*Os03g08020*	TTTCACTCTTGGTGTGAAGCAGAT	GACTTCCTTCACGATTTCATCGTAA	Exon 1 and Exon 2	103	Ji et al., 2014
EXPnarsai	*Os07g02340*	ATGGGCAGAAGTCGAAGATG	TCTCAGAGGTGGTGCAGATG	Exon 1 and Exon 3	144	self-made sequence
RBR2	*Os11g0533500*	TGGGAGATCTTGAAGGGTTG	GCTTCCCAATCTGACCCATA	Exon 3 and Exon 4	116	self-made sequence
CDKB1-1	*Os01g0897000*	AACCGGTGTTGACATTTGGT	GTTACTCCAGGCCACTGCTC	Exon 4 and Exon 5	150	self-made sequence
CDKB2-1	*Os08g0512600*	GCTCGTTCACTGTCCCTCTC	GTGGCCAACTCAGCAAAAAT	Exon 2 and E3-E4-jn	145	self-made sequence
CYCA3-2	*Os12g0581800*	TAACTGCAATTCGCGACAAG	GGAGGTATGACGCAGGGATA	Exon 6 and Exon 7	90	self-made sequence
CATA	*Os02g0115700*	GCCGGATAGACAGGAGAGGT	CCAACGACTCATCACACTGG	Exon 3 and E3-E4-jn	119	self-made sequence
CATB	*Os06g0727200*	TCATGCACAGGGATGAAGAG	CCAGCCTGTTGGAAATTGTT	Exon 4 and Exon 6	148	self-made sequence
CATC	*Os03g0131200*	GCATCTGGCTCTCCTACTGG	CTCCTTACATGCTCGGCTTC	Exon 5 and Exon 6 + UTR	90	self-made sequence
APX1	*Os03g0285700*	GCTACCAAGGGTTCTGACCA	CAAGGTCCCTCAAAACCAGA	Exon 4 and Exon 5	137	self-made sequence
APX2	*Os07g0694700*	AAGTGACAAAGCCCTCATGG	TCCTCAGCAAATCCCAGTTC	Exon 7 and Exon 8	132	self-made sequence
APX3	*Os04g0223300*	CGGGCATCAAGATTGCTATT	CAACTCCGGCAAGCTGATAC	Exon 2 and Exon 3	93	self-made sequence
APX8	*Os02g0553200*	TACTAAGGATGGGCCTGGTG	AAGATCCTGGTCCCTTTGCT	Exon 7 and Exon 8	109	self-made sequence
MnSOD	*Os05g0323900*	TGTTGGGAATTGATGTCTGG	CAAGCAGTCGCATTTTCGTA	Exon 5 and Exon 6	133	self-made sequence
FeSOD	*Os06g0143000*	CACAAAATGCCATCAGTCCA	TTCGCCTGTCATCCTTGTAA	Exon 5 and E7-E8-jn	102	self-made sequence
CuZnSODchl.	*Os08g0561700*	CGAATGGGTGCATATCAACA	CAATGGTTGCCTCAGCTACA	Exon 3 and Exon 5	138	self-made sequence
CuZnSODcyt.	*Os03g0351500*	AAGTGTCTCTGGCCTCAAGC	TTGTAGTGTGGCCCAGTTGA	Exon 2 and E2-E3-jn	96	self-made sequence
CuZnSODper.	*Os03g0219200*	GGCAGTTGTTGTTCATGCTG	CCAATTCTTGCTCCTGCATT	Exon 5 and Exon 6	90	self-made sequence

845 **Table A2.** Reverse transcription quantitative PCR parameters according to the Minimum Information
846 for publication of Quantitative real-time PCR Experiments (MIQE) guidelines derived from Bustin *et*
847 *al*., 2009.

Sample/Template	
Source	*Oryza sativa* leaves in a hydroponic culture
Method of preservation	Harvest in liquid nitrogen, storage at -80 °C
Storage time (if appropriate)	Maximum two weeks
Handling	Frozen
Extraction method	Protocol described in Valledor *et al.* (2014)
RNA: DNA-free	Turbo DNA-*free*™ Kit
	Use of intron-spanning primers whenever possible
	Verification of single peak on dissociation curves
RNA: concentration	NanoDrop® ND-1000 spectrophotometer
RNA: integrity	Agilent 2100 Bioanalyzer system.
Assay optimisation/validation	
Accession number	Table S1
Amplicon details	Exon location and amplicon size: Table S1
Primer sequence	Table S1
In silico	Primer-BLAST (https://blast.ncbi.nlm.nih.gov/Blast.cgi)
Empirical	Primer concentrations of 300 nM
	Annealing temperature of 60 °C
Priming conditions	Combination of oligo-dT primers and random hexamers
PCR efficiency	Dilution curves (slope, deviation)
Linear dynamic range	Samples are within the range of the efficiency curve
RT and qPCR	
Protocols	Turbo DNA-*free*™ Kit
	PrimeScript™ RT Reagent Kit
	QuantiNova SYBR Green
	As described in the Materials and methods section
Reagents	As described in the materials and methods section
NTC	Cq and dissociation curve verification
Data analysis	
Specialist software	7500 Fast System Sequence Detection Software, version 1.4.0
Statistical justification	As described in the Materials and methods section and Table legends
Transparent, validated normalisation	Minimum four references genes selected using the GrayNorm algorithm
	As described in the Materials and methods section

848

849

850

Table A3. The fold change expression level of superoxide dismutase isoforms at 10 µM Cd exposure of different leaf growth zones expressed relative to the same zone under control conditions (set at 1.00). Asterisks indicate a significant upregulation under Cd exposure across all zones together for that isoform (Two-way ANOVA; p-value < 0.05). The *CuZnSOD* isoforms are present in the chloroplastic (chl.), cytosol (cyt.) and peroxisomes (per.).

	LOCATION				
GENE	**D**	**T_1**	**E**	**T_2**	**M**
MnSOD	0.89 ± 0.01	0.88 ± 0.02	1.07 ± 0.06	0.93 ± 0.06	1.23 ± 0.05
FeSOD	0.95 ± 0.07	1.06 ± 0.1	1.06 ± 0.06	1.16 ± 0.03	1.12 ± 0.12
*CuZnSODchl.**	1.01 ± 0.03	1.03 ± 0.04	1.14 ± 0.11	1.39 ± 0.12	1.19 ± 0.04
CuZnSODcyt.	0.92 ± 0.07	0.98 ± 0.05	1.07 ± 0.13	0.72 ± 0.08	0.9 ± 0.01
CuZnSODper.	0.81 ± 0.08	0.75 ± 0.03	1.18 ± 0.35	1.15 ± 0.23	1.17 ± 0.25